DOI: 10.1002/chem.200902575

Self-Association of Bis-Dendritic Organogelators: The Effect of Dendritic Architecture on Multivalent Cooperative Interactions

Myungeun Seo, Jung Hak Kim, Jisung Kim, Nojin Park, Jeyoung Park, and Sang Youl Kim*[a]

Abstract: A series of bis-dendritic gelators consisting of a benzamide dendron and an alkyl dendron were synthesized to investigate the dendritic effect on self-assembly. The gelators with a first-generation benzamide (benzamide-**G1**) dendron or a first-generation alkyl (alkyl-**G1**) dendron formed stable gels in most aromatic solvents, and their self-assembled fibrillar networks were imaged by electron microscopy. The unbranched molecule (**G0**-**G0**) or the molecule possessing a second-generation benzamide (benzamide-**G2**) dendron did not form gels. Differential scanning calorimetry, powder X-ray diffraction, and Fourier transform IR studies revealed that introduction of a dendritic branch strongly affected the molecular packing as well as the strength of intermolecular interactions. Furthermore, concentration-dependent diffusion coefficient measurements and the evaluation of association constants by ^{1}H NMR spectroscopy indicated that bis-dendritic gelators with a benzamide-**G1** dendron possessed high association constants and formed large aggregates, whereas molecules with a single benzamide formed dimers in chloroform. The formation of self-assembled fibrillar networks was driven by the multivalent and cooperative hydrogen bonding observed in the benzamide-**G1** dendrons. π–π stacking of aromatic groups and van der Waals interactions between alkyl chains also played roles in the self-assembly process, thus indicating that a spatial balance between two dendrons is important.

Keywords: benzamide · dendrimers · gels · hydrogen bonds · self-assembly

Introduction

Dendritic architectures provide multiple reactive sites on the interior and periphery of macromolecules together with precise control over the number and chemical composition of these sites.[1] The development of synthetic strategies for dendritic molecules has focused on supramolecular chemistry in which a well-defined molecular structure is necessary for the design of intermolecular interactions.[2] Various dendritic hybrid structures have been described, including dendritic wedges,[3–5] dendritic amphiphiles,[6] diblock dendrimers,[7] and dendron-containing block copolymers.[8–10] Globular dendritic structures have been found useful for the formation of supramolecular assemblies.

Dendritic architectures have also been used for constructing organogelators, which, at low concentrations, immobilize organic liquids by forming self-assembled fibrillar networks.[11] In most cases, hydrogen-bonding moieties introduced at the focal point or along the branches[12–15] of the dendron complement nonpolar interactions in the bulky nonpolar dendron to stabilize the network.[16] On the other hand, Stupp and co-workers pioneered self-assembly of dendritic gelators containing hydroxyl groups at the periphery and demonstrated various functionalities can be embedded in the architecture.[17]

Introducing hydrogen-bonding moieties at the periphery of a dendron allows cooperative multivalent bonding between many proximal moieties. In nature, multivalent interactions between ligands and receptors are frequently observed in supramolecular assemblies[18] because cooperative binding enhances ligand binding affinity, known as the 'dendritic effect'.[19] Quantitative descriptions of the self-association process are crucial for understanding the dendritic effect at the molecular level. Because the gelation process is, in principle, an aggregation process involving a large number of molecules, it requires models that are more so-

[a] Dr. M. Seo, J. H. Kim, J. Kim, N. Park, J. Park, Prof. S. Y. Kim
Department of Chemistry, KAIST
Gwahangno 335, Yuseong-gu, Daejeon 305-701 (Korea)
Fax: (+82) 42-350-8177
E-mail: kimsy@kaist.ac.kr

Supporting information for this article is available on the WWW under http://dx.doi.org/10.1002/chem.200902575.

phisticated than the conventional dimerization model used to describe binding between host and guest molecules. The indefinite self-association models described by Martin[20] have been applied to the gelation process in a few reports,[21] although these models were originally developed to describe π–π stacking interactions between adjacent DNA base pairs.

To investigate the molecular basis for the dendritic effect in self-assembly, we synthesized a series of bis-dendritic molecules consisting of benzamide and alkyl dendrons. The benzamide moiety, a hydrogen-bonding motif used in crystal engineering, was selected to investigate the effect of branches on the molecular structure.[22] The hydrogen-bonding patterns of benzamide are described by a combination of two supramolecular synthons, $R_2^2(8)$ (a face-to-face hydrogen bond utilizing *syn*-hydrogen atoms) and $C(4)$ (a side-to-side hydrogen bond utilizing *anti*-hydrogen atoms), which yield a two-dimensional hydrogen-bonded network.[23] A previous attempt to construct an organogelator with the benzamide moiety resulted in a gelator with modest gelation properties due to the tendency of benzamide to form highly crystalline aggregates.[24] Modifying benzamide at the *ortho* position with a trifluoromethyl group improved the solubility while maintaining the hydrogen-bonding ability.[25] By introducing the modified benzamide moiety at the dendritic periphery, we were able to make noncovalently bound polymeric nanoparticles by means of supramolecular chain collapse assisted by hydrogen bonding.[26]

The association of the dendritic benzamide moieties is expected to be multivalent and cooperative because they contain multiple hydrogen-bonding sites, each of which forms a two-dimensional hydrogen bond. The alkyl dendron should also be important in forming aggregates because it provides van der Waals interaction between alkyl chains and protects benzamide hydrogen bonds from the solvent. The spatial balance between two dendrons may play another role in self-assembly, by balancing hydrogen bonding and van der Waals interaction and allowing physical gelation at low concentrations.

In this study, the self-association of bis-dendritic gelators was investigated by varying the generation of the dendron on either side of the bis-dendritic molecules. By employing various characterization techniques for xerogel and solution states, we show that the existence of a dendritic branch produced a physical gel consisting of nanoscopic fibers, but the gelation properties and intermolecular interactions were found to be strongly dependent on the generation. The self-association of the bis-dendritic gelators was fit to the indefinite self-association models, and the results clearly demonstrated that the dendritic effect plays a key role in the self-association of bis-dendritic gelators by providing multivalent and cooperative interactions.

Results and Discussion

Synthesis: A small library of bis-dendritic molecules, consisting of benzamide dendrons and alkyl dendrons, was prepared by following the synthetic routes depicted in Scheme 1.

Previously, we described the unusual crystal growth of 4-dodecyloxy-2-trifluoromethylbenzamide (**G0**-**G0**), which forms parallelogrammatic pipes by means of a polymorphic transition.[25] Based on the molecular architecture of **G0**-**G0**, the first-generation benzamide dendron (benzamide-**G1**) was synthesized by nucleophilic aromatic substitution (S_NAr) between the 4-nitro-2-trifluoromethylbenzonitrile (**1**) and 3,5-dihydroxybenzyl alcohol.[26] The main product resulted from displacement of the nitro group (which was activated by the electron-withdrawing nitrile and trifluoromethyl groups) by phenoxides in the 3,5-dihydroxybenzyl alcohol. Small quantities of side products consisting of 1- or 3-substituted compounds were also produced. Hydrolysis of the nitrile groups to benzamide groups and esterification of the benzyl alcohol with 1-dodecanoic acid yielded the desired compound, **G1**-**G0**.

To synthesize the second-generation benzamide dendron (benzamide-**G2**), conversion of benzyl alcohol into benzyl bromide was performed using the convergent approach described for the synthesis of Fréchet-type benzyl ether dendrons.[27] Reaction of **4** with carbon tetrabromide and triphenylphosphine in THF produced the desired compound (**7**). Benzamide-**G2** was obtained by further S_N2 reaction of **7** with 3,5-dihydroxybenzyl alcohol and hydrolysis of the nitrile groups into benzamide groups. Esterification between the benzyl alcohol and 1-dodecanoic acid yielded the desired **G2**-**G0**.

3,5-Bis(dodecyloxy)benzoic acid,[28] a double-alkyl-tailed compound joined by a carboxylic acid moiety at the focal point, was chosen for the construction of **G1**-**G1**. In the case of **G0**-**G1**, synthesis began with dimethyl 5-hydroxyisophthalate. After introduction of the benzamide group, hydrolysis of the ester groups liberated the acid moieties, and subsequent esterification with 1-dodecanol yielded the desired compound. Interestingly, during the hydrolysis of the nitrile group, 3-(4-carbamoyl-3-trifluoromethylphenoxy)-5-methoxycarbonylbenzoic acid containing one free carboxylic acid group was produced as a side product. The compound was also converted into 5-(4-carbamoyl-3-trifluoromethylphenoxy)isophthalic acid (**18**).

Thermal properties: The thermal transitions of the products were investigated by differential scanning calorimetry (DSC) and polarized optical microscopy (POM) equipped with a heating stage. Figure 1a–e shows DSC thermograms of the bis-dendritic gelator molecules during the first heating cycle. Thermograms were recorded at a heating rate of $10\,^{\circ}C\,min^{-1}$ under a N_2 atmosphere. Thermograms of the first and second heating/cooling cycles are provided in the Supporting Information. Table 1 shows a summary of the transition temperatures and corresponding transition enthalpies.

According to the previous analysis, **G0**-**G0** possesses two polymorphic forms, all-*trans* **L** and *gauche*-rich **S**.[25a] The DSC thermogram of a solid of **G0**-**G0** from toluene solution

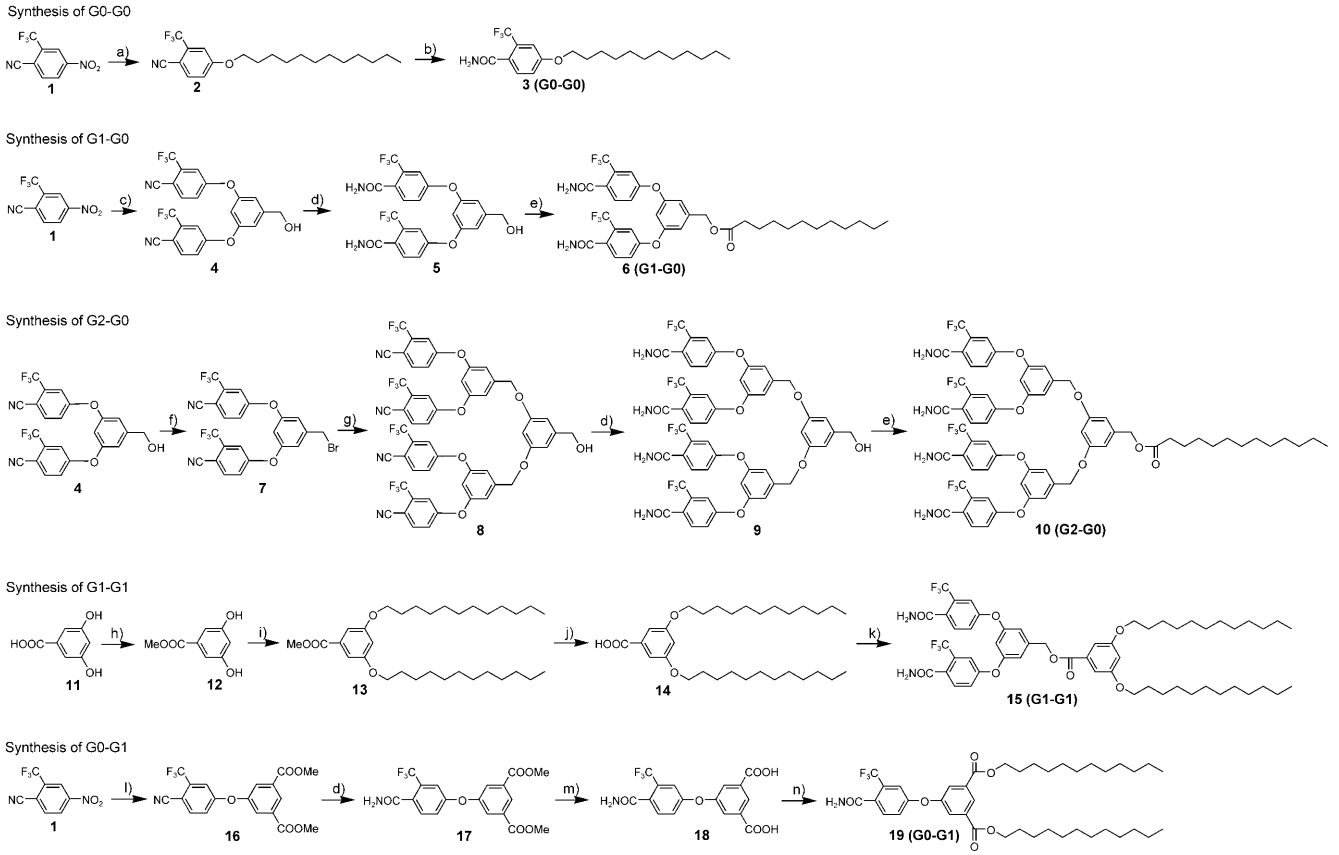

Scheme 1. Synthetic routes to the bis-dendritic molecules. a) 1-Dodecanol, NaH, THF, reflux, 15 h. b) KOH, H_2O, EtOH, 60 °C, 10 h. c) 3,5-Dihydroxybenzyl alcohol, K_2CO_3, DMSO, RT, 10 h. d) K_2CO_3, H_2O_2 (aq), DMSO, RT, 2 h. e) 1-Dodecanoic acid, EDC, DMAP, THF, RT, 4 h. f) CBr_4, Ph_3P, THF, RT, 30 min. g) 3,5-Dihydroxybenzyl alcohol, K_2CO_3, acetone, reflux, 48 h. h) H_2SO_4 (cat.), MeOH, reflux, 20 h. i) 1-Bromododecane, K_2CO_3, acetone, reflux, 48 h. j) KOH, EtOH, reflux, 2 h. k) **5**, EDC, DMAP, THF, RT, 4 h. l) Dimethyl 5-hydroxyisophthalate, K_2CO_3, DMSO, RT, 3 h. m) LiOH, THF/MeOH/H_2O 6:3:1, RT, 4 h. n) 1-Dodecanol, EDC, DMAP, DMF, RT, 18 h. (EDC = 1-ethyl-3-(3-dimethylaminopropyl)carbodiimide hydrochloride, DMAP = 4-dimethylaminopyridine.)

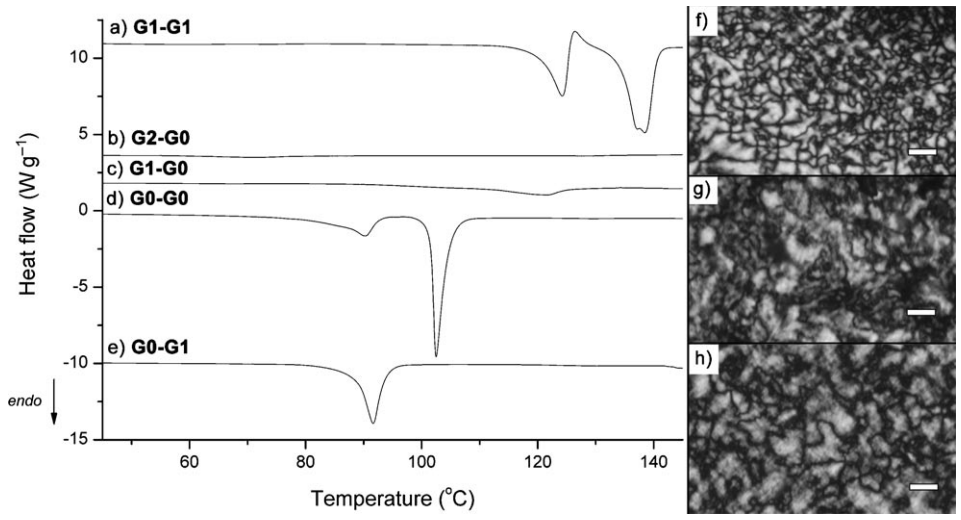

Figure 1. DSC thermograms of the bis-dendritic gelator molecules a) **G1**-**G1**, b) **G2**-**G0**, c) **G1**-**G0**, d) **G0**-**G0**, and e) **G0**-**G1** during the first heating cycle. Thermograms were recorded at a heating rate of 10 °C min^{-1} in a N_2 atmosphere. POM images of compounds f) **G1**-**G1**, g) **G1**-**G0**, and h) **G0**-**G1** showing liquid-crystalline textures. Scale bars represent 20 μm.

(Figure 1d) shows that the compound possesses an **S** polymorphic form, an intercalated bilayer lamellar structure that consists of stronger face-to-face hydrogen bonds between benzamide groups and a more *gauche*-rich configuration of alkyl chains than the **L** polymorphic form. It seems that the melting transition at 103 °C corresponds to the cleavage of hydrogen bonds between benzamide groups and the premelting transition at 90 °C corresponds to the transition between alkyl-chain configurations. No morphological change was observed between 90 and 103 °C.

Compared to the thermal behavior of **G0**-**G0**, **G1**-**G0**

Table 1. Thermal properties of the bis-dendritic gelators **G*n*-G*m***.[a]

Entry	1st heating	1st cooling	2nd heating	2nd cooling
G1-G1	124.26 (28.78) 138.39 (52.96)	n.d.[b]	90.60 (−26.59) 136.85 (35.90)	n.d.[b]
G2-G0	n.d.[b]	n.d.[b]	n.d.[b]	n.d.[b]
G1-G0	121.42 (21.69)	n.d.[b]	n.d.[b]	n.d.[b]
G0-G0	90.26 (35.71) 102.50 (91.34)	79.20 (−84.97)	79.81 (1.79) 102.67 (92.81)	78.17 (−84.06)
G0-G1	91.65 (64.70)	49.20 (−48.50)	71.41 (29.28) 88.21 (16.57)	49.20 (−49.83)

[a] Temperatures are expressed in °C. Transition enthalpies [$J g^{-1}$] are shown in parentheses. Positive and negative values represent endothermic and exothermic transitions, respectively. [b] n.d.: not determined.

showed a very weak and broad transition at 121 °C that was classified as a melting transition (Figure 1c). When observed by POM, **G1-G0** showed a morphological change to a liquid-crystalline state depicted in Figure 1g. The texture persisted as the sample was cooled to room temperature. However, the sample melted completely above 125 °C and remained amorphous when subjected to further temperature changes. These results suggest that the initial alkyl-chain transition was followed by cleavage of hydrogen bonds between benzamide groups. An increase in the melting transition temperature with a decrease in the corresponding transition enthalpy suggested that the benzamide-**G1** dendron increased the amount of intermolecular interactions but decreased the crystallinity.

POM imaging indicated that **G2-G0** became isotropic at 92 °C. However, **G2-G0** did not show any detectable thermal transitions in the DSC thermograms during the first and second heating/cooling cycles (Figure 1b). This result implies that the benzamide groups in the benzamide-**G2** dendron of **G2-G0** do not interact cooperatively and do not increase the strength of intermolecular interactions even though the dendron has four potential interaction sites nearby. The benzamide groups in the benzamide-**G2** dendron appeared to have different orientations due to steric repulsion, and the intermolecular association of the benzamide-**G2** dendron seemed to involve several molecules. Thus, the melting transition temperature of **G2-G0** mainly reflects monomeric dissociation of benzamide groups.

In Figure 1a, **G1-G1** was characterized by the highest melting transition temperature in the series, 139 °C, which suggests the importance of spatial balance in the molecular structure. The melting transition was accompanied by another premelting transition at 125 °C, and POM analysis indicated that a liquid-crystalline state similar to that observed for **G1-G0** appeared during the premelting transition temperature (Figure 1g). The state became isotropic above 140 °C. During the second heating cycle, the compound showed an exothermic transition corresponding to crystallization at 91 °C and an endothermic transition corresponding to melting at 137 °C.

The melting transition temperature of **G0-G1** was observed at 92 °C during the first heating cycle (Figure 1e), and crystallization was also observed at 49 °C on cooling. During the second heating cycle, **G0-G1** showed two endothermic transitions consisting of premelting (71 °C) and melting (88 °C), which were very similar to the transitions in the thermogram of **G1-G1** during the first heating cycle. Similar liquid crystalline textures were also observed between the temperatures (Figure 1h). These results suggest that introduction of a branch on either side of the dendrimer broke the symmetry of crystalline **G0-G0** and promoted anisotropic intermolecular interactions. Whereas an increase in the number of benzamide groups enhanced the intermolecular association to a certain extent, reflected in an increase in melting transition temperature, an appropriate number of alkyl chains was also important for stabilizing hydrogen bonds.

Gelation properties: All bis-dendritic molecules were subjected to gelation tests in a variety of organic solvents. Each compound was combined with solvent in a screw-capped sample tube, and heated until the solid fully dissolved. The solution was then cooled to room temperature, and gelation was monitored by inverting the sample tube to see whether the solution flows or not. The observed gelation behavior of each solution is summarized in Table 2.

Table 2. Gelation of organic solvents by the bis-dendritic gelators **G*n*-G*m***.[a]

	G0-G0	G1-G0	G2-G0	G1-G1	G0-G1
n-hexane	P	I	I	G	G
benzene	S	P	P	G	S
toluene	S	G	P	G	S
xylene	S	G	P	G	S
chlorobenzene	S	G	P	G	S
1-butanol	S	S	I	G	S
chloroform	S	S	I	S	S
ethyl acetate	S	S	S	S	S
acetonitrile	S	S	S	S	S
DMSO	S	S	S	S	S

[a] Tested at 3 mg mL^{-1} concentration. G: gel. P: precipitation. S: solution. I: insoluble.

Compound **G0-G0** showed good solubility in a range of organic solvents with the exception of *n*-hexane, in which crystallization occurred. While **G0-G0** showed no gelation in any solvent tested, compounds possessing a single branch on the benzamide dendron (**G1-G0**), the alkyl dendron (**G0-G1**), or both dendrons (**G1-G1**) formed a gel in most nonpolar solvents. Compound **G1-G0** gelled in the aromatic solvents toluene, ethylbenzene, and chlorobenzene but was insoluble in benzene or *n*-hexane. Compound **G1-G0** dissolved in the polar solvents such as ethyl acetate and DMSO presumably due to the disruption of hydrogen bonding. However, **G2-G0** showed much poorer solubility in aromatic solvents, in which precipitation occurred when the heated solution was cooled to room temperature. No gelation properties were observed for **G2-G0**. Again, these trends in gelation properties indicate that nonspecific hydro-

gen bonding in **G2-G0** involved a number of molecules. As a result, insoluble aggregates were produced because the relatively small alkyl groups could not provide the necessary solubility in nonpolar solvents.

Compound **G1-G1** showed not only enhanced solubility relative to **G1-G0**, but also underwent gelation in the widest range of solvents, including aromatic solvents, *n*-hexane, and 1-butanol. The origin of the wide gelation window of **G1-G1** was attributed to the well-matched spatial balance between the benzamide dendron and the alkyl dendron, which cooperatively provided strong intermolecular interactions consisting of hydrogen bonding, π–π stacking, and van der Waals interactions between alkyl chains.

Compound **G0-G1** showed the best solubility in the series because the relatively large alkyl dendron seemed to improve solubility in organic solvents. It only formed a stable gel in *n*-hexane, presumably due to the favorable packing of the alkyl-**G1** dendron. It should be noted that the compounds possessing benzamide-**G1** dendrons formed gels in aromatic solvents, and the compounds possessing alkyl-**G1** dendrons formed gels in *n*-hexane.

The microscopic structure of the gel was investigated by field-emission SEM (FE-SEM). Figure 2 shows representative FE-SEM images of the xerogel of **G1-G0**, **G1-G1**, and **G0-G1** formed in various solvents (additional SEM and TEM images are presented in the Supporting Information).

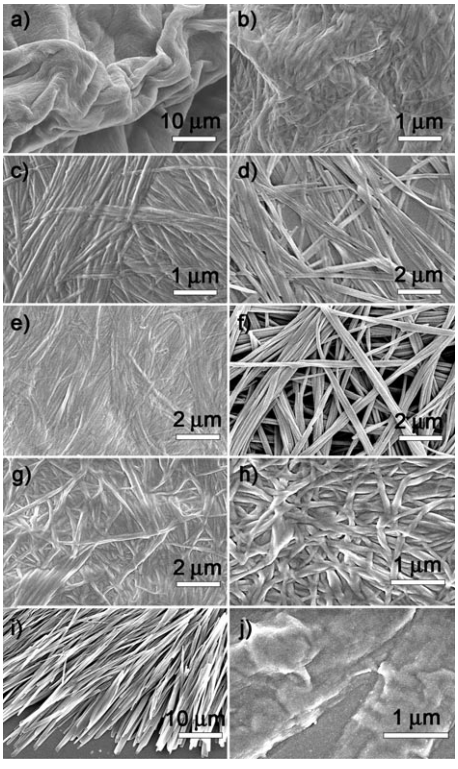

Figure 2. FE-SEM images of the xerogel of **G1-G0**, **G1-G1**, and **G0-G1** formed in various solvents (a–g), and solids of **G0-G1**, **G0-G0**, and **G2-G0** obtained by evaporation of a solution drop on a Si wafer. a),b) **G1-G0** in toluene. c) **G1-G0** in xylene. d) **G1-G1** in benzene. e) **G1-G1** in toluene. f) **G1-G1** in 1-butanol. g) **G0-G1** in *n*-hexane. h) **G0-G1** in toluene. i) **G0-G0** in toluene. j) **G2-G0** in chlorobenzene.

These images clearly show that well-defined nanofibers were formed by self-assembly of the bis-dendritic gelators that contained at least one branch on one side of the bis-dendritic gelator, which yielded a physically cross-linked fibrillar network in three dimensions. The diameter of the nanofibers ranged from several dozen to more than a hundred nanometers, which suggests that they are actually bundles of smaller fibers. Interestingly, the self-assembled structures of **G1-G1** shown in Figure 2d–f look like ribbons rather than fibers: they are straight and rarely twisted. Compared with **G1-G0** and **G0-G1**, the spatially well-balanced molecular structure of **G1-G1** seemed to provide more favorable packing of alkyl chains, strengthening and straightening the self-assembled structure while reducing the curvature. An SEM image of solid **G0-G1** obtained by evaporation of toluene also revealed a highly entangled fibrillar network. This observation implied that self-association of **G0-G1** also occurs in toluene, similar to **G1-G0** and **G1-G1**, although the concentration at which the microscopic structure appears has not been determined. Compound **G0-G0**, obtained by evaporation of toluene, only produced crystalline solids as depicted in Figure 2i. It seems that the introduction of a branch was essential for producing one-dimensional growth of self-assembled structures instead of three-dimensional growth of crystalline solids. The **G2-G0** precipitate formed in toluene showed a two-dimensional sheetlike morphology on the micrometer scale, as shown in Figure 2j.

Analysis of self-assembled structures: The dependence of the self-association properties on dendron generation for the bis-dendritic gelator molecules was further investigated for **G1-G1**, **G1-G0**, **G0-G0**, and **G0-G1** in toluene, but not for **G2-G0** because it failed to form self-assembled structures in comparable conditions. Figure 3 shows powder

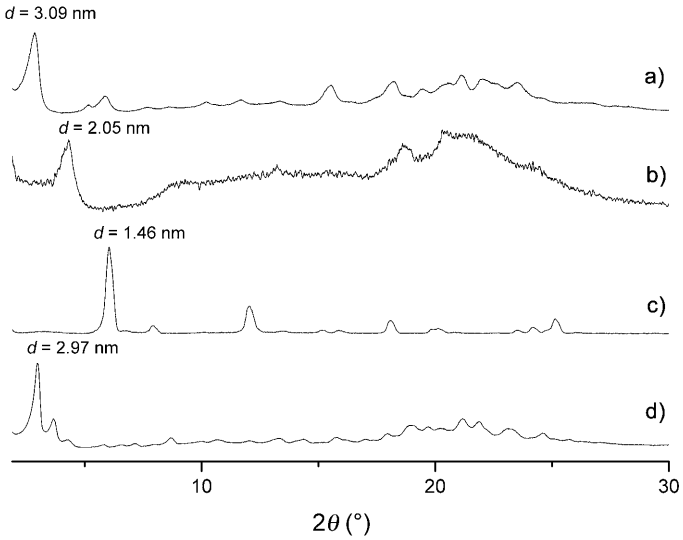

Figure 3. Powder XRD patterns of the compounds obtained from toluene. Patterns were normalized to the intensities of the first peaks. a) Xerogel of **G1-G1**. b) Xerogel of **G1-G0**. c) Solid of **G0-G0** obtained by evaporation. d) Solid of **G0-G1** obtained by evaporation.

XRD patterns of the xerogels of **G1**-**G1** and **G1**-**G0** in toluene, and the solids of **G0**-**G0** and **G0**-**G1** obtained by evaporation of toluene.

The powder XRD patterns of **G1**-**G1**, **G1**-**G0**, and **G0**-**G1** show characteristics of self-assembled materials consisting of lamellar structures with different layer spacings, evident in the sharp peaks that appear at small angles and the broad peaks at wide angles. Compared with these XRD patterns, crystalline **G0**-**G0** shows more refined signals accompanied by higher-order reflections. The diffraction pattern of **G1**-**G0** was interpreted as an intercalated bilayer lamellar structure with the layer spacing of $d=2.05$ nm. However, this spacing is quite small considering that the extended length of the molecule is around 2.5 nm. Therefore it appears that the alkyl chains that filled the void between the relatively large benzamide dendrons adopted the highly disordered configuration. The intensity of the XRD pattern was relatively weak, indicating poor periodicity in the self-assembled structure and supporting the presumed presence of disorder among alkyl groups.

In contrast with **G1**-**G0**, **G1**-**G1** showed much more refined signals with strong intensities that reflected balance in the molecular structure of **G1**-**G1**. Moreover, a peak at 2.9° and following higher-order reflections indicated the much longer lamellar spacing of $d=3.09$ nm than that of **G1**-**G0**. Introduction of the alkyl-**G1** dendron therefore provided better packing of the alkyl groups and increased van der Waals interactions. The straight and rarely twisted morphology of **G1**-**G1** compared with the fibrous **G1**-**G0** could be also attributed to balance in the molecular structure.

The effect of the alkyl-**G1** dendron is also evident in **G0**-**G1**, which showed an XRD peak at 3.0° corresponding to the layer spacing of $d=2.97$ nm. The observation that layer spacing of **G0**-**G1** is slightly smaller than **G1**-**G1** but much larger than **G1**-**G0** suggests that the packing of alkyl chains determines the periodicity of the bilayer structure. XRD patterns of **G0**-**G1** obtained from a sample in toluene and a xerogel of *n*-hexane were indistinguishable, which indicated that they possessed identical self-assembled structures. In a dilute solution in toluene, however, hydrogen bonding between single benzamide groups of **G0**-**G1** may be too weak to compensate for the entropy loss of alkyl chains, and macroscopic gelation may not occur.

To gain insight into the driving force for gelation, FTIR studies were conducted. Figure 4 shows the characteristic IR absorption of **G1**-**G1** and **G1**-**G0** xerogels in toluene, and **G0**-**G0** and **G0**-**G1** solids obtained by evaporation of the toluene. The spectra in Figure 4a–d show $\nu(NH_2)$ stretching vibration frequencies at 3500–3100 cm^{-1} and $\nu(CH_2)$ stretching frequencies at 3000–2800 cm^{-1}, and the spectra in Figure 4e–h show $\nu(C{=}O)$ stretching vibration frequencies of esters at 1750–1700 cm^{-1}; amide I for $\nu(C{=}O)$ stretching and amide II for N–H in-plane bending coupled to a C–N stretching of benzamides at 1700–1550 cm^{-1}; and $\delta(CH_2)$ scissoring deformations at approximately 1470 cm^{-1}.[29,30]

Benzamides are known to exhibit two bands corresponding to asymmetric $\nu_{as}(NH_2)$ stretching at approximately

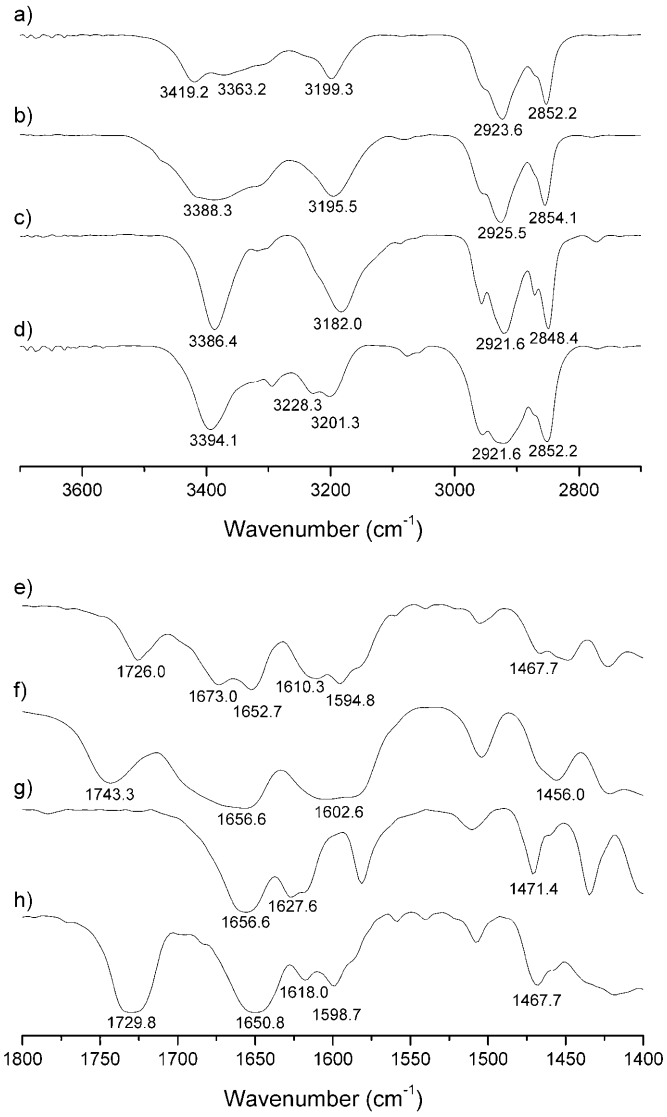

Figure 4. FTIR spectra of the compounds obtained from toluene evaporation. a),e) Xerogel of **G1**-**G1**. b),f) Xerogel of **G1**-**G0**. c),g) Solid of **G0**-**G0** obtained by evaporation. d),h) Solid of **G0**-**G1** obtained by evaporation.

3400 cm^{-1} and symmetric $\nu_s(NH_2)$ stretching at approximately 3200 cm^{-1}.[29] Analysis of **G0**-**G0** in toluene again confirms the presence of the **S** polymorphic form as suggested by the DSC and powder XRD study.[25] In contrast with **G0**-**G0**, the compounds with benzamide-**G1** dendrons (**G1**-**G1** and **G1**-**G0**) showed much broader and redshifted $\nu_{as}(NH_2)$ stretching frequencies, which indicated the presence of strong hydrogen bonds between N–H and C=O.[28] This observation, also supported by broadened bands of amide I and amide II shown at 1700–1550 cm^{-1} in **G1**-**G1** and **G1**-**G0**, suggests that hydrogen bonding is the driving force for gelation. It was noticed that frequencies of $\nu_s(NH_2)$ stretching were blueshifted to 3196 (**G1**-**G0**) and 3199 cm^{-1} (**G1**-**G1**) compared to those of **G0**-**G0** (3182 cm^{-1}), presumably due to the looser molecular packing in **G1** series. These values are

comparable to those found in the **L** polymorphic form of **G0-G0** (3197 cm^{-1}).[25a]

A vibration band corresponding to $\nu_{as}(NH_2)$ stretching of **G0-G1** also shows a redshifted shoulder, but the frequency of the main band appears at 3394 cm^{-1}, indicating the weakness of hydrogen bonds in **G0-G1**. The same tendency is observed for the frequency of $\nu_s(NH_2)$ stretching, which was blueshifted (3201 cm^{-1}) compared to the corresponding band in **G0-G0**. It seems that **G0-G1** does not provide optimal geometry for hydrogen bonding between benzamide groups. The bulky alkyl-**G1** dendron is large enough to induce steric hindrance between the benzamide groups and the favorable packing of alkyl chains is thermodynamically more important than the benzamide hydrogen bonding for stabilizing the self-assembled structure.

Analysis of bands corresponding to the methylene vibrations provides more information on the packing of alkyl groups. The CH_2 asymmetric $\nu_{as}(CH_2)$ and symmetric $\nu_s(CH_2)$ stretching vibrations of alkyl groups generally show strong absorptions around 2918–2928 cm^{-1} and 2850–2860 cm^{-1}, respectively.[30] Inclusion of *gauche* conformations in the alkyl group results in a blueshift in bands at frequencies 2923–2928 and 2852–2860 cm^{-1}. In the series, **G1-G0** shows the highest frequency values for $\nu_{as}(CH_2)$ (2926 cm^{-1}) and $\nu_s(CH_2)$ (2854 cm^{-1}) stretching vibrations, thus confirming that the spatially unbalanced alkyl chains are highly disordered, as suggested by powder XRD study. This trend is also evident in $\delta(CH_2)$ scissoring deformation frequencies, for which inclusion of *gauche* conformations results in a redshift because **G1-G0** exhibits the lowest frequency, at 1456 cm^{-1}. Apparently, the ordering of alkyl chains in **G0-G1** is comparable to **G1-G1** and even **G0-G0**, based on the band frequencies of $\nu_{as}(CH_2)$, $\nu_s(CH_2)$, and $\delta(CH_2)$ vibrations. This observation highlights the importance of alkyl chains packing in the self-assembled structure. Again, an FTIR spectrum of **G0-G1** obtained from the *n*-hexane xerogel was identical to the spectrum shown in Figure 4d and h.

Examination of self-assembly in solution: In addition to characterizing the self-assembly of bis-dendritic gelators in the xerogel state, self-assembly behavior of bis-dendritic gelators was examined directly in solution using concentration-dependent pulsed-field gradient spin-echo (PGSE) NMR spectroscopy[31] and concentration-dependent ^1H solution NMR spectroscopy measurements.[21,32] Although deuterated toluene would have been the ideal solvent, chemical shift overlap between residual solvent protons and the amide and aromatic protons of the compound proved to be problematic. Deuterated chloroform ($CDCl_3$) was therefore used because it provides a moderately nonpolar environment and does not interrupt hydrogen bonding. All the bis-dendritic gelator molecules except for **G2-G0** were soluble in $CDCl_3$ and provided clear and distinct chemical shifts in the concentration ranges of 1–100 mM.

By employing PGSE NMR spectroscopy techniques, diffusion coefficients of the bis-dendritic gelators were determined at several concentrations. Because the Einstein–Stokes equation predicts that a diffusion coefficient is inversely proportional to the hydrodynamic radius of a species in solution, the diffusion coefficients obtained can be used to estimate the degree of self-association in solution. Figure 5a shows measured diffusion coefficients of the bis-dendritic gelators.

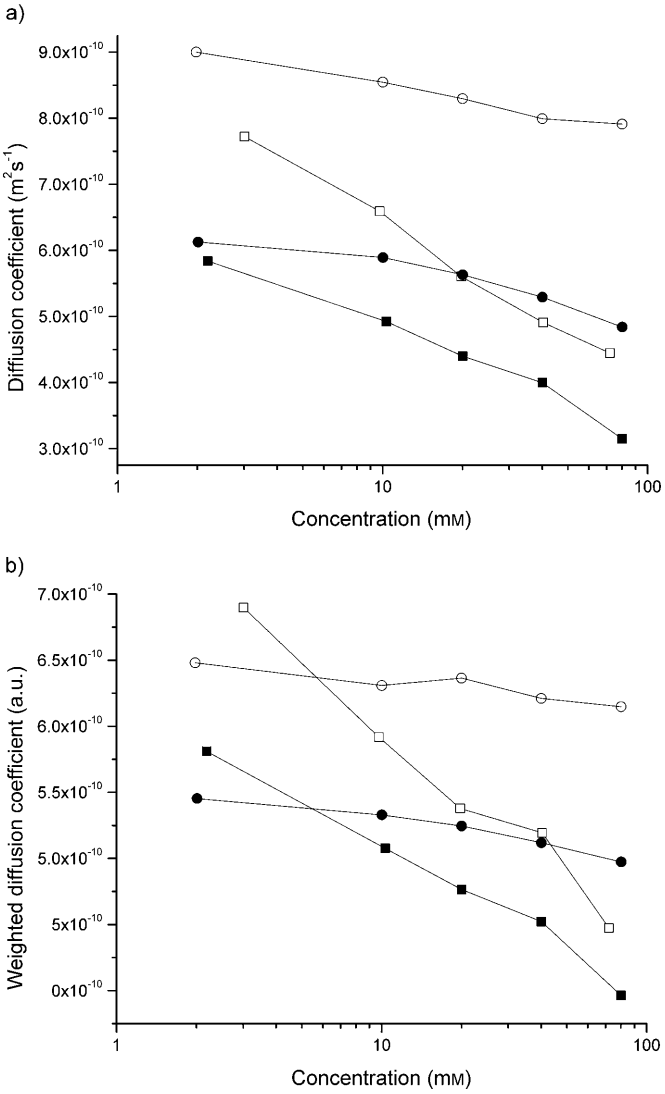

Figure 5. a) Measured diffusion coefficients of the bis-dendritic gelators. b) Viscosity corrected and molecular-weight weighted diffusion coefficients of the bis-dendritic gelators. Measurements were performed in $CDCl_3$ at 25 °C. ■: **G1-G1**; □: **G1-G0**; ●: **G0-G1**; ○: **G0-G0**.

The relationship between the diffusion coefficient and the concentration is clearly different for the **G1** and **G0** series. In the **G1** series, diffusion coefficients varied from 5.8×10^{-10} to 3.1×10^{-10} m^2s^{-1} for **G1-G1**, and from 7.7×10^{-10} to 4.4×10^{-10} m^2s^{-1} for **G1-G0**. In contrast, the change of diffusion coefficient was much smaller in **G0** series, ranging from 6.1×10^{-10} to 4.8×10^{-10} m^2s^{-1} for **G0-G1** and from 9.0×10^{-10} to 7.9×10^{-10} m^2s^{-1} for **G0-G0**. The large difference between

the **G1** and **G0** series suggests that the association modes of the two series are different.

To clarify the effect of a dendritic branch on benzamide dendron self-association, the diffusion coefficients shown in Figure 5a were corrected by solution viscosity determined by the diffusion coefficient of residual chloroform. In addition, diffusion coefficients were normalized by the cubed root of the bis-dendritic gelator molecular weight to remove the effect of molecular volume (assuming that density is uniform across compounds and that molecular volume is proportional to molecular weight). Again, the slopes shown in Figure 5b clearly indicate that **G1**-**G1** and **G1**-**G0** form large aggregates at high concentrations, whereas **G0**-**G1** and **G0**-**G0** appear to form dimeric species. These results imply that the dendritic branch in the benzamide dendron is key to the indefinite self-association and the formation of self-assembled fibrillar networks.

Association constants of the bis-dendritic gelators were evaluated by concentration-dependent solution ^{1}H NMR spectroscopy experiments in deuterated chloroform. Figure 6 shows representative ^{1}H NMR spectra of the bis-dendritic gelator molecules **G1**-**G1**, **G1**-**G0**, **G0**-**G0**, and **G0**-**G1** at various concentrations. Peak assignments for each molecule are also given. In the spectra, signals 1–3 appear consistently at $\delta = 7$–8 ppm and were assigned to the aromatic protons in the benzamide phenyl group. Other aromatic protons in the "branching" phenyl rings were also assigned for each generation of dendrons. Aliphatic protons on the carbon adjacent to the ethereal oxygen or on the carbonyl carbon appeared at chemical shifts of $\delta \approx 4$ ppm or $\delta \approx 2.3$ ppm, respectively. Below $\delta = 2$ ppm, peaks were assigned to aliphatic protons in the alkyl chains.

The amide protons in the benzamide group exhibited two signals (NH1 and NH2) indicating restricted rotation of the NH_2 group around its N–CO bond due to hydrogen bonding.[33] By considering that benzamides form two-dimensional hydrogen-bonding networks consisting of face-to-face hydrogen bonds by means of H_{syn} atoms and side-to-side hydrogen bonding by means of H_{anti} atoms, the peak shifted further downfield (NH1) was assigned to H_{syn} and the upfield peak (NH2) was assigned to H_{anti}. As the concentration increased, NH1 and NH2 shifted further downfield, and the distance between NH1 and NH2 increased. The downfield shift indicates proton deshielding by interaction with hydro-

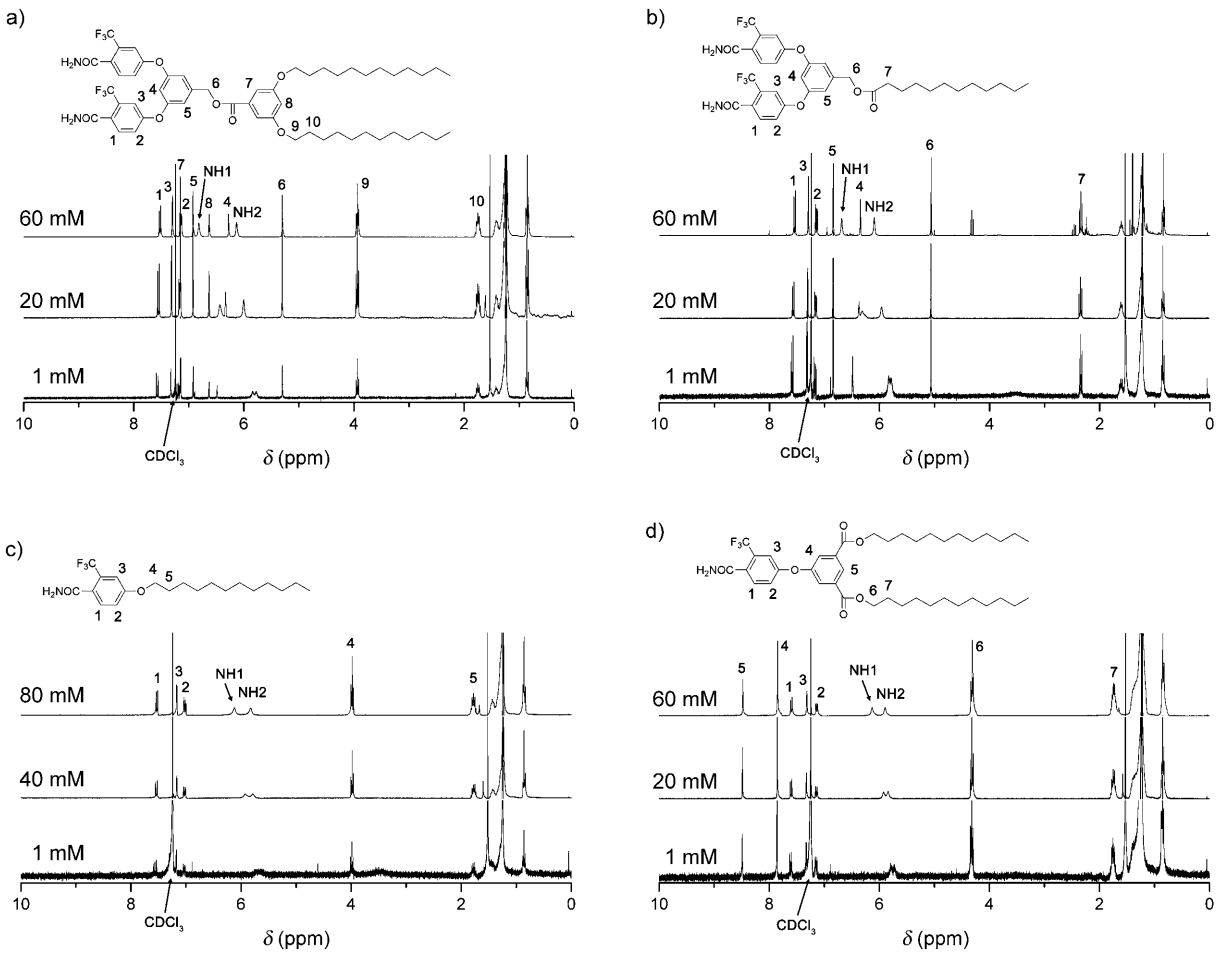

Figure 6. ^{1}H NMR spectra of the bis-dendritic gelator molecules at various concentrations (300 MHz, $CDCl_3$, 25 °C). a) **G1**-**G1**. b) **G1**-**G0**. c) **G0**-**G0**. d) **G0**-**G1**.

gen acceptors (carbonyl oxygen in this case), consistent with an increase in intermolecular hydrogen bonding among benzamide groups. Notably, the extent of the downfield shift was much larger in molecules containing a benzamide-**G1** dendron than in molecules containing a single benzamide, which indicated that the presence of the dendron enhanced the hydrogen bonding. NH1 and NH2 signals in molecules containing a single benzamide merged at a concentration of approximately 10 mM but split when the concentration was further decreased. Due to merging, concentration-dependent chemical shifts of NH2 for **G0**-**G0** and **G0**-**G1** yielded scattered data points.

The measured dependences of NH1 and NH2 NMR spectroscopy shifts on bis-dendritic gelator concentration were fit using association models described by Martin.[20] Based on the results of diffusion coefficient measurements, Equal K (EK) and cooperative Equal K (coEK) models were applied to the **G1**-**G1** and **G1**-**G0** data as indefinite self-association models, and a dimeric (DIM) model was applied to the **G0**-**G1** and **G0**-**G0** data. Whereas the DIM model describes the fraction of dimeric aggregates and non-aggregated molecules in the solution with association constant K_2, the coEK model accounts for nearest-neighbor interactions and represents indefinite association with $K_E = K_2/\rho = K_3 = K_4 = \ldots = K_n$ ($\rho = K_2/K_E$). If $\rho = 1$, the coEK model converges to the EK model, which does not differentiate between the nucleation and growth processes (isodesmic growth).[20,34] Figure 7a and b show concentration-dependent ^{1}H NMR spectroscopy shifts of NH1 and NH2 for **G1**-**G1**, **G1**-**G0**, **G0**-**G0**, and **G0**-**G1**, fitted to either the EK model (**G1** series) or the DIM model (**G0** series). Figure 7c and d show fits of the **G1** series using the coEK model.

Table 3 shows a summary of the association constants and fit parameters of the bis-dendritic gelators. Both models fit well to all data sets for the benzamide-**G1** series, but comparison of two models based on Akaike's information criterion method and the extra sum-of-squares F test indicated that the simpler EK model (with 3 parameters) is more likely to be correct than the more complicated coEK model (with 4 parameters).[35] These results suggest that the self-assembly of the benzamide-**G1** dendrons follows the isodesmic growth mechanism and the strength of secondary interactions between monomers in the polymer chains is unaffected by the length of the chain.[34] The benzamide association constants estimated for the benzamide-**G1** dendrons were in the range of 16–28 M^{-1} determined by the EK model. These values are comparable to association constants reported for toluene gelators in chloroform,[21c] and, as suggested previously, the association constants are expected to be much higher in toluene be-

Table 3. Association constants of the bis-dendritic gelators **G*n*-G*m***.[a]

	G1-**G1** NH1	**G1**-**G1** NH2	**G1**-**G0** NH1	**G1**-**G0** NH2
		EK model		
K_E [M^{-1}]	24	28	22	16
P_α [ppm]	5.73	5.80	5.78	5.81
P_ξ [ppm]	7.87	6.42	7.82	6.54
fitting error[b]	3×10^{-3}	3×10^{-3}	1.2×10^{-2}	3×10^{-3}
		coEK model		
K_E [M^{-1}]	49	38	39	39
ρ	0.240	1.00	0.431	0.860
K_2 [M^{-1}]	17	55	17	34
P_α [ppm]	5.84	5.78	5.83	5.79
P_ξ [ppm]	7.31	6.37	7.41	6.36
fitting error[b]	7×10^{-3}	3×10^{-3}	1×10^{-2}	4×10^{-3}
	G0-**G0** NH1	**G0**-**G0** NH2	**G0**-**G1** NH1	**G0**-**G1** NH2
		DIM model		
K_2 [M^{-1}]	2	3	5	6
P_α [ppm]	5.64	5.72	5.71	5.77
P_λ [ppm]	8.34	6.15	7.22	6.18
fitting error[b]	3×10^{-3}	3×10^{-3}	1×10^{-3}	1×10^{-3}

[a] For definitions of the symbols, see the Experimental Section. [b] The fitting error was calculated as $\sum_{n=1}^{m} |(\text{residual})_i|^2$, in which the residual is defined by the difference between the experimental and the model fit.

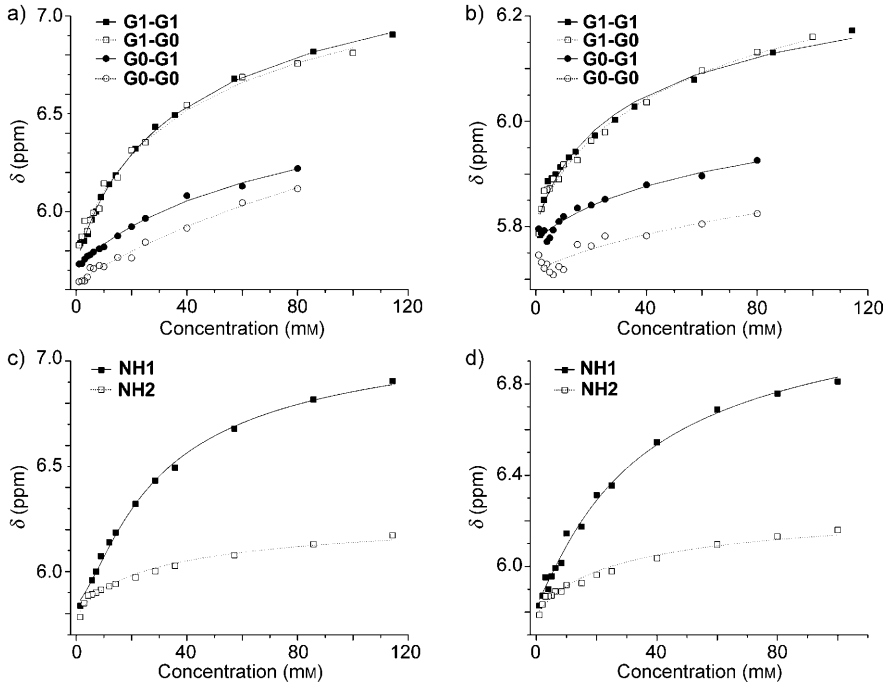

Figure 7. Concentration-dependent ^{1}H NMR spectroscopy shifts of NH1 and NH2 of the bis-dendritic gelator molecules (300 MHz, $CDCl_3$). a) NH1. b) NH2. Measured data points are shown as squares (**G1** series) and circles (**G0** series), and fits are shown as lines (**G1** series, EK model) and dots (**G0** series, DIM model). c) Fits of **G1**-**G1** based on the coEK model. d) Fits of **G1**-**G0** based on the coEK model.

cause chloroform provides a considerably more polar environment than toluene. Observation of larger association constants for **G1**-**G1** than for **G1**-**G0** implies that stabilization of hydrogen bonding in nonpolar environments by the sterically bulky alkyl-**G1** dendron is also important for self-association.

Association constants of the **G0** series corresponding to dimerization were much smaller than those of the **G1** series, and ranged from 2–6 M^{-1}. Considering that molecules consisting of the benzamide-**G1** dendron possess twice as many benzamide groups at a given concentration, the association constants of the **G0** series are still smaller than half of those of the **G1** series. Therefore, introduction of the benzamide-**G1** dendron significantly enhances the strength and cooperativity of hydrogen bonding. For the system discussed here, this effect was explained by a reduction in entropy loss during successive association processes of the benzamide-**G1** dendron. When one of the benzamide moieties in the dendron participates in aggregation by means of hydrogen bonding, the next association by means of hydrogen bonding will be more facile due to the restriction on translational degrees of freedom. On the other hand, dissociation of a single benzamide from the aggregate will not be entropically favorable because it does not result in complete dissociation from the aggregate.[36] Again, association constants for **G0**-**G1** were larger than those of **G0**-**G0**.

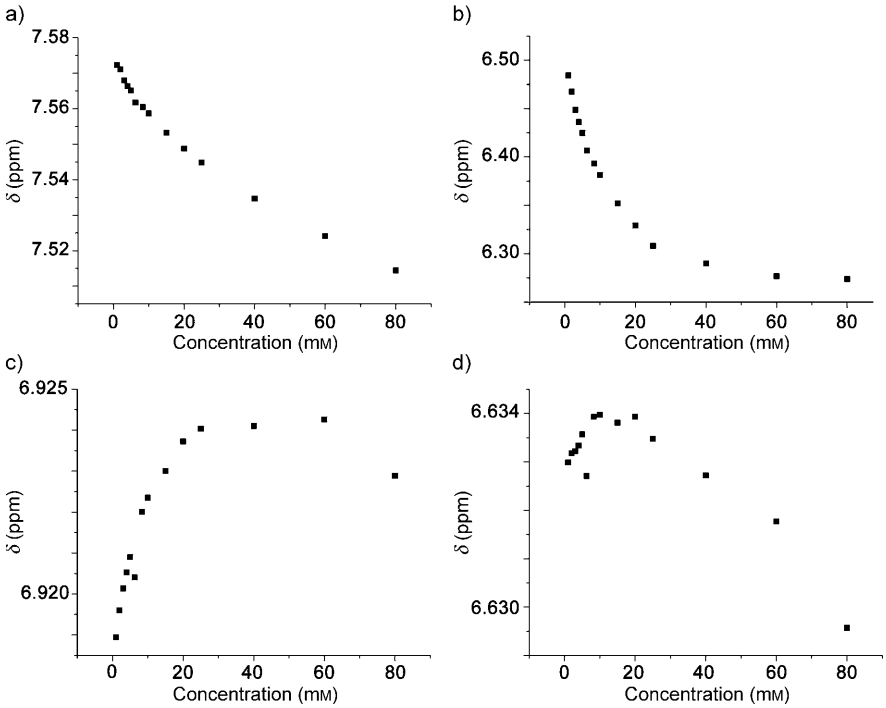

Figure 8. Concentration-dependent ^{1}H NMR spectroscopy shifts of protons in **G1**-**G1** (300 MHz, $CDCl_3$). a) H1. b) H4. c) H5. d) H8.

The aromatic and benzylic protons also showed a dependence of chemical shift on concentration. Peaks 1–3, corresponding to aromatic protons in the benzamide phenyl group, shifted upfield as the concentration increased. This shift was attributed to increased shielding of protons from π–π stacking between proximal aromatic rings.[20,37] Peak 4 for the benzamide-**G1** dendrons (**G1**-**G1** and **G1**-**G0**) also shifted upfield, because the H4 proton is located between two aromatic rings in the benzamide-**G1** dendron and experiences the increased shielding upon aggregation.

In contrast, the H5 and H6 protons in **G1**-**G1** and **G1**-**G0** show only a slight shift downfield at low concentrations, reach maximal chemical shifts at 20–25 mM, and then shift upfield at higher concentrations. This trend is also observed for the H7 and H8 protons in **G1**-**G1** but not for H5 and H6 protons in **G0**-**G1**. Figure 8 shows the concentration-dependent ^{1}H NMR spectroscopy shifts of H1, H4, H5, and H8 protons in **G1**-**G1**.

These results suggest that the branching phenyl rings behave differently from the benzamide phenyl rings for the molecules containing a benzamide-**G1** dendron. A possible explanation for the different behavior between types of aromatics is that a branching phenyl ring is nearly perpendicular to the benzamide phenyl ring and tends to form separate weak stacking systems with the aid of van der Waals interactions between the alkyl chains. Thus, the mechanism of gelation in **G1**-**G1** and **G1**-**G0** can be described as association of the benzamide-**G1** dendron by means of hydrogen bonding and π–π stacking, and continued growth of aggregates by the participation of branching phenyl rings and alkyl chains through π–π stacking and van der Waals interactions.

This mechanism also explains why **G1**-**G1** forms the most stable gels in a variety of solvents, because **G1**-**G1** achieves the strongest intermolecular interactions by spatially balancing hydrogen bonding, π–π stacking, and van der Waals interactions. Compound **G1**-**G0** has weaker π–π stacking and van der Waals interactions and its gelation relies to a great extent on hydrogen bonding, which restricts the range of solvents conducive to gelation. On the contrary, **G0**-**G1** relies on mainly van der Waals interactions for gelation, so stable gels form only in *n*-hexane, in which the interaction between alkyl chains is maximized. Compound **G0**-**G0** may have a balanced molecular structure, but its intermolecular interactions are weak in solution and crystallization is favored over gelation in the solid state. Figure 9 summarizes the conclusion that self-assembly of the bis-dendritic gelators can be reliably tuned by adjusting the generation number of each dendron.

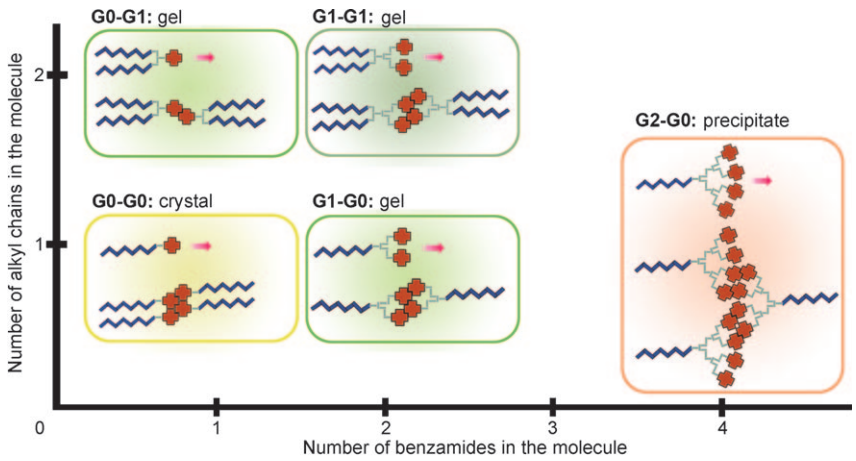

Figure 9. Relationship between the structure and properties of the bis-dendritic gelator molecules.

Conclusion

We prepared a series of bis-dendritic gelator molecules consisting of benzamide and alkyl dendrons to study the relationship between macroscopic gelation (self-assembled fibrillar networks) and the molecular-level intermolecular interactions. The generation-dependent gelation behavior reported here demonstrates that multivalent cooperativity among peripherally interacting groups in dendritic architectures strongly affects the nature of intermolecular association. Investigation of the influence of alkyl chains revealed that spatial balance in the molecular structure is also very important for balancing the intermolecular interactions and for allowing gelation in a range of solvents.

Experimental Section

General: All starting materials were obtained from commercial suppliers and were used without further purification. Syntheses of **1**, **2**, **3**, **4**, and **5** were published elsewhere.[25a,26] Compound **14**[28] was synthesized following reported procedures. Synthesized compounds were structurally verified by NMR spectroscopy. $MgSO_4$ was used to dry all organic solutions during workup procedures. Analytical TLC was performed on Kieselgel 60 F-254 precoated TLC plates. Silica 60 (230–400 mesh) from Merck was used for flash chromatography. The ^1H and ^{13}C NMR spectra were recorded on a Bruker Fourier Transform AVANCE 400 spectrometer. Chemical shifts were expressed in part per million using residual solvent protons. High-resolution mass spectra (HRMS) of the compounds were obtained on a VG Autospec Ultima mass spectrometer using the electroionization method and on a Bruker MicroTOF-Q tandem mass spectrometer using the electrospray ionization method. DSC studies were performed on a TA Q100 calorimeter. Samples were measured in aluminum hermetic cells under a N_2 atmosphere at a heating rate of $10\,^\circ C\,min^{-1}$. POM studies were performed on a Nikon Eclipse ME600 microscope equipped with a Mettler-Toledo FP82 hot stage and an FP90 central processor. SEM studies were performed on a Philips XL30S FE-SEM instrument for gold-sputtered samples. TEM studies were performed on an EM 912 OMEGA TEM instrument for samples on a carbon-coated copper TEM grid without staining. Powder XRD patterns were obtained with a Rigaku D/MAX-RB diffractometer using a scan speed of $0.05^\circ\,min^{-1}$ and with sampling width of 0.01°, using $Cu_{K\alpha}$ ($\lambda = 0.154$ nm) as a light source. FTIR spectra were recorded on a Bruker EQUINOX-55 spectrometer using KBr pellets.

Compound 6 (G1-G0): Compound **5** (0.4 g, 0.778 mmol), 1-dodecanoic acid (0.467 g, 2.333 mmol), and DMAP (0.285 g, 2.333 mol) were dissolved in THF (40 mL) and placed in a 100 mL one-necked round-bottomed flask. The reaction mixture was stirred at 0 °C for 30 min. EDC (0.285 g, 2.333 mmol) was added into the flask and stirred for an additional 30 min. The reaction mixture was warmed up to room temperature and was stirred for 3 h. Then, the reaction mixture was filtered, washed with 0.1 M HCl (aq), 0.1 M $NaHCO_3$, and brine. The organic layer was dried and evaporated in a rotary evaporator. The excess dodecanoic acid was removed by precipitation in *n*-hexane (0.491 g, 88.3 %). M.p. 125 °C; ^1H NMR (400 MHz, $CDCl_3$, 25 °C): $\delta = 7.56$ (d, $^1J(H,H) = 8.2$ Hz, 2H; ArH), 7.30 (d, $^1J(H,H) = 2.3$ Hz, 2H; ArH), 7.41 (dd, $^1J(H,H) = 8.5$ Hz, $^2J(H,H) = 2.3$ Hz, 2H; ArH), 6.84 (d, $^1J(H,H) = 2.0$ Hz, 2H; ArH), 6.74 (s, 2H; NH of amide), 6.44 (t, $^1J(H,H) = 2.3$ Hz, 1H; OH), 6.00 (s, 2H; another NH of amide), 5.06 (s, 2H; CH_2OH), 2.34 (t, $^1J(H,H) = 7.4$ Hz, 2H; $C{=}OCH_2$), 1.61 (t, $^1J(H,H) = 7.0$ Hz, 2H; $C{=}OCH_2CH_2$), 1.24 (m, 16H), 0.85 ppm (t, $^1J(H,H) = 6.2$ Hz, 3H; CH_3); ^{13}C NMR (100 MHz, $CDCl_3$, 25 °C): $\delta =$ 173.4, 169.7, 157.5, 140.7, 130.7, 130.4, 129.3 (q, $^2J(C,F) = 32.6$ Hz), 126.9, 122.9 (q, $^1J(C,F) = 272.2$ Hz), 121.9, 117.3 (q, $^3J(C,F) = 5.1$ Hz), 64.8, 34.1, 31.8, 29.5–29.1, 24.8, 22.6, 14.0 ppm; ESIMS: *m/z*: calcd: 697.2707; found: 697.2707 [M^+]; calcd: 719.2526; found: 719.5310 [M+Na^+] ; elemental analysis calcd (%) for $C_{35}H_{38}F_6N_2O_6$: C 60.34, H 5.50, F 16.36, N 4.02, O 13.78; found: C 61.88, H 5.49, N 3.86.

Compound 7: Compound **4** (1.216 g, 2.091 mmol), carbon tetrabromide (2.022 g, 6.097 mmol), and triphenylphosphine (1.600 g, 6.100 mmol) were placed in a 100 mL three-necked round-bottomed flask. Under nitrogen purging, THF (50 mL) was added into the flask. The reaction mixture was stirred for 30 min at room temperature. Then the mixture was poured into the excess water, and then extracted with ethyl acetate (EA). The organic layer was dried and evaporated in a rotary evaporator. The desired product was purified by flash column chromatography (EA/hexane (Hx) 1:3 to 1:2) to yield a yellow solid (0.4 g, 35.3 %). M.p. $< 40\,^\circ C$; ^1H NMR (400 MHz, $CDCl_3$, 25 °C): $\delta = 7.80$ (d, $^1J(H,H) = 8.6$ Hz, 2H; ArH), 7.37 (d, $^1J(H,H) = 2.5$ Hz, 2H; ArH), 7.21 (dd, $^1J(H,H) =$ 8.6 Hz, $^2J(H,H) = 2.5$ Hz, 2H; ArH), 7.00 (d, $^1J(H,H) = 2.2$ Hz, 2H; ArH), 6.73 (t, $^1J(H,H) = 2.2$ Hz, 1H; ArH), 4.42 ppm (s, 2H; CH_2Br); ^{13}C NMR (100 MHz, $CDCl_3$, 25 °C): $\delta = 160.2$, 155.9, 142.7, 136.9, 135.3 (q, $^2J(C,F) = 33.0$ Hz), 121.8 (q, $^1J(C,F) = 272.7$ Hz), 120.5, 116.5 (q, $^3J(C,F) = 4.8$ Hz), 115.0, 111.9, 104.4, 31.0 ppm; ESIMS: *m/z*: calcd: 540.9981; found: 540.9988 [M+H^+]; elemental analysis calcd (%) for $C_{23}H_{11}BrF_6N_2O_2$: C 51.04, H 2.05, Br 14.76, F 21.06, N 5.18, O 5.91; found: C 47.03, H 1.83, N 4.48.

Compound 8: Compound **7** (0.506 g, 0.935 mmol), 3,5-dihydroxybenzyl alcohol (0.066 g, 0.468 mmol), potassium carbonate (0.161 g, 1.169 mmol), and [18]crown-6 (0.024 g, 0.092 mmol) were placed in a 25 mL three-necked round-bottomed flask and stirred. Acetone (5 mL) was added into the flask and the reaction mixture was refluxed under nitrogen purging for 24 h. Then the reaction mixture was cooled to room temperature, filtered, and concentrated in a rotary evaporator. The mixture was dissolved again in EA, washed with water and brine, and dried. The organic layer was evaporated in a rotary evaporator. The desired product was purified by flash column chromatography (EA/Hx 1:1) to yield a yellow viscous liquid (0.365 g, 36.8 %). M.p. 65 °C; ^1H NMR (400 MHz, $CDCl_3$, 25 °C): $\delta = 7.76$ (d, $^1J(H,H) = 8.6$ Hz, 4H; ArH), 7.36 (d, $^1J(H,H) = 2.4$ Hz, 4H; ArH), 7.19 (dd, $^1J(H,H) = 8.6$ Hz, $^2J(H,H) = 2.5$ Hz, 4H; ArH), 7.03

(d, ^1J(H,H) = 2.1 Hz, 4H; ArH), 6.76 (t, ^1J(H,H) = 2.1 Hz, 2H; ArH), 6.58 (d, ^1J(H,H) = 2.1 Hz, 2H; ArH), 6.42 (t, ^1J(H,H) = 2.1 Hz, 1H; ArH), 5.05 (s, 4H; CH_2O), 4.61 ppm (s, 2H; CH_2OH); ^{13}C NMR (100 MHz, $CDCl_3$, 25 °C): δ = 160.2, 155.9, 142.7, 136.9, 135.3 (q, ^2J(C,F) = 33.0 Hz), 121.8 (q, ^1J(C,F) = 272.7 Hz), 120.5, 116.5 (q, ^3J(C,F) = 4.8 Hz), 115.0, 111.9, 104.4, 31.0 ppm; ESIMS: *m/z*: calcd: 1061.1839; found: 1061.1907 [M+H$^+$]; elemental analysis calcd for $C_{53}H_{28}F_{12}N_4O_7$: C 60.01, H 2.66, F 21.49, N 5.28, O 10.56; found: C 59.77, H 2.92, N 4.91.

Compound 9: Compound **9** was synthesized from **8** (0.147 g, 0.139 mmol) using the same protocol as that for **5** (0.125 g, 89.4%). M.p. 120 °C; ^{1}H NMR (400 MHz, [D$_6$]DMSO, 25 °C): δ = 7.91 (s, 2H; NH of amide), 7.56 (s, 2H; another NH of amide), 7.55 (s, 2H; ArH), 7.37 (d, ^1J(H,H) = 2.0 Hz, 2H; ArH), 7.32 (dd, ^1J(H,H) = 8.5 Hz, ^2J(H,H) = 2.0 Hz, 2H; ArH), 6.86 (d, ^1J(H,H) = 1.5 Hz, 2H; ArH), 6.73 (s, 1H; ArH), 5.36 (t, ^1J(H,H) = 5.7 Hz, 1H; OH), 4.48 ppm (d, ^1J(H,H) = 5.5 Hz, 2H; CH_2OH); ^{13}C NMR (100 MHz, [D$_6$]DMSO, 25 °C): δ = 168.5, 156.9, 147.6, 132.0, 130.8, 127.8 (q, ^2J(C,F) = 32 Hz), 127.3, 123.2 (q, ^1J(C,F) = 272.2 Hz), 121.7, 116.2, 112.6, 108.8, 62.1 ppm; ESIMS: *m/z*: calcd: 1133.2262; found: 1133.2408 [M+H$^+$]; elemental analysis calcd (%) for $C_{53}H_{35}F_{12}N_4O_{11}$: C 56.19, H 3.20, F 20.12, N 4.95, O 15.54; found: C 54.52, H 3.12, N 4.90.

Compound 10 (G2-G0): Compound **10** was synthesized from **9** (5 g, 14.07 mmol) using the same protocol as that for **6** (1.11 g, 21.1%). M.p. 88 °C; ^{1}H NMR (400 MHz, [D$_6$]DMSO, 25 °C): δ = 7.89 (s, 4H; NH of amide), 7.57 (s, 4H; ArH), 7.55 (s, 4H; another NH of amide), 7.39 (d, ^1J(H,H) = 2.2 Hz, 4H; ArH), 7.33 (dd, ^1J(H,H) = 8.4 Hz, ^2J(H,H) = 2.2 Hz, 4H; ArH), 7.00 (d, ^1J(H,H) = 2.0 Hz, 2H; ArH), 6.78 (t, ^1J(H,H) = 1.9 Hz, 2H; ArH), 6.59 (d, ^1J(H,H) = 1.8 Hz, ArH), 6.57 (s, 1H; ArH), 5.09 (s, 4H; **G1**-CH_2O), 4.98 (s, 2H; **G2**-CH_2O), 2.31 (t, ^1J(H,H) = 7.3 Hz, 2H; C=OCH_2), 1.50 (t, ^1J(H,H) = 6.5 Hz, 2H; C=OCH_2CH_2), 1.18 (m, 16H), 0.81 ppm (t, ^1J(H,H) = 6.5 Hz, 3H; CH_3); ^{13}C NMR (100 MHz, [D$_6$]DMSO, 25 °C): δ = 172.7, 168.4, 159.1, 156.9, 156.6, 141.6, 138.8, 132.1, 130.7, 127.9 (q, ^2J(C,F) = 31.9 Hz), 123.1 (q, ^1J(C,F) = 272.2 Hz), 121.6, 116.2 (q, ^3J(C,F) = 5.1 Hz), 113.8, 109.5, 106.8, 101.3, 68.3, 64.9, 33.4, 31.3, 28.9–28.4, 24.4, 22.1, 13.9 ppm; ESIMS: *m/z*: calcd: 1337.3752; found: 1337.3682 [M+Na$^+$]; elemental analysis calcd (%) for $C_{65}H_{58}F_{12}N_4O_{12}$: C 59.36, H 4.45, F 17.33, N 4.26, O 14.60; found: C 58.44, H 5.26, N 4.12.

Compound 15 (G1-G1): Compound **15** was synthesized from **6** (0.2 g, 14.07 mmol) and **14** using the same protocol as that for **6** (0.219 g, 56.9%). M.p. 138 °C; ^{1}H NMR (400 MHz, $CDCl_3$, 25 °C): δ = 7.54 (d, ^1J(H,H) = 8.4 Hz, 2H; ArH), 7.31 (d, ^1J(H,H) = 2.3 Hz, 2H; ArH), 7.41 (dt, ^1J(H,H) = 2.3 Hz, ^2J(H,H) = 4.1 Hz, 4H; ArH), 6.92 (d, ^1J(H,H) = 2.3 Hz, 2H; ArH), 6.63 (t, ^1J(H,H) = 2.3 Hz, 1H; ArH), 6.61 (s, 2H; NH of amide), 6.31 (t, ^1J(H,H) = 2.2 Hz, 1H; ArH), 6.07 (s, 2H; another NH of amide), 5.30 (s, 2H; CH_2OC=O), 3.94 (t, ^1J(H,H) = 6.5 Hz, 4H; O=$COCH_2$), 1.75 (m, ^1J(H,H) = 7.8 Hz, 4H; O=$COCH_2CH_2$), 1.42 (m, ^1J(H,H) = 8.0 Hz, 4H; C=O$CH_2CH_2CH_2$), 1.24 (m, 32H), 0.86 ppm (t, ^1J(H,H) = 6.6 Hz, 6H; CH_3); ^{13}C NMR (100 MHz, $CDCl_3$, 25 °C): δ = 169.5, 166.1, 160.2, 157.8, 157.4, 140.6, 131.3, 130.7, 130.5, 129.4 (q, ^2J(C,F) = 32.7 Hz), 122.9 (q, ^1J(C,F) = 272.2 Hz), 122.1, 117.5, 113.9, 1082, 107.9, 106.6, 68.4, 65.5, 31.9, 29.6–29.2, 26.0, 22.7, 14.1 ppm; ESIMS: *m/z*: calcd: 987.4953; found: 987.4980 [M+H$^+$]; elemental analysis calcd (%) for $C_{54}H_{68}F_6N_2O_8$: C 65.70, H 6.94, F 11.55, N 2.84, O 12.97; found: C 62.83, H 5.92, N 3.65.

Compound 16: Compound **1** (1.028 g, 4.758 mmol) and dimethyl 3-hydroxyisophthlate (1 g, 4.758 mmol) were dissolved in DMSO (12 mL) and placed in a 25 mL one-necked round-bottomed flask. Potassium carbonate (0.658 g, 4.758 mmol) was added into the flask and the solution was stirred at room temperature for 3 h. Then the solution was poured into water (150 mL), and filtered to obtained a white solid that was dried under vacuum (1.481 g, 79.9%). M.p. 133 °C; ^{1}H NMR (400 MHz, [D$_6$]DMSO, 25 °C): δ = 8.33 (s, 1H; ArH), 8.14 (d, ^1J(H,H) = 8.6 Hz, 1H; ArH), 7.93 (s, 2H; ArH), 7.66 (d, ^1J(H,H) = 2.0 Hz, 1H; ArH), 7.53 (s, 1H; ArH), 7.40 (dd, ^1J(H,H) = 8.6 Hz, ^2J(H,H) = 2.3 Hz, 1H; ArH), 3.87 ppm (s, 6H; CH_3); ^{13}C NMR (100 MHz, [D$_6$]DMSO, 25 °C): δ = 164.5, 160.4, 154.6, 137.9, 133.2 (q, ^2J(C,F) = 32.0 Hz), 132.6, 126.4, 125.2, 122.0 (q, ^1J(C,F) = 272.2 Hz), 121.4, 117.2 (q, ^3J(C,F) = 4.8 Hz), 115.3, 102.9, 52.7 ppm; EIMS: *m/z*: calcd: 379.0668; found: 379.0667 [M^+]; elemental analysis calcd (%) for $C_{18}H_{12}F_3NO_5$: C 57.00, H 3.19, F 15.03, N 3.69, O 21.09; found: C 56.95, H 3.22, N 3.65.

Compound 17: Compound **16** (0.5 g, 1.318 mmol) was dissolved in DMSO (3 mL) and placed in a 10 mL one-necked round-bottomed flask. At 0 °C, potassium carbonate (0.2 g, 1.447 mmol) and 30% H_2O_2 (aq) (0.9 mL) were added into the flask. The reaction mixture was warmed up to room temperature and additional DMSO (5 mL) was added. After 21 h, the reaction mixture was poured into water (100 mL). The white solid was filtered and dried under vacuum (0.182 g, 34.7%). M.p. 186 °C; ^{1}H NMR (400 MHz, [D$_6$]DMSO, 25 °C): δ = 8.35 (s, 1H; ArH), 7.98 (s, 1H; NH of amide), 7.79 (s, 1H; another NH of amide), 7.60 (d, ^1J(H,H) = 8.1 Hz, 2H; ArH), 7.51 (s, 1H; ArH), 7.39 (dd, ^1J(H,H) = 8.4 Hz, ^2J(H,H) = 2.3 Hz, 1H; ArH), 3.87 ppm (s, 6H; CH_3); ^{13}C NMR (100 MHz, [D$_6$]DMSO, 25 °C): δ = 168.3, 164.6, 156.5, 156.2, 132.8, 132.3, 130.9, 127.8 (q, ^2J(C,F) = 32.1 Hz), 126.4, 124.4, 123.1 (q, ^1J(C,F) = 272.3 Hz), 122.3, 117.2 (q, ^3J(C,F) = 4.5 Hz), 52.7 ppm; EIMS: *m/z*: calcd: 397.077; found: 3397.0774 [M^+]; elemental analysis calcd (%) for $C_{18}H_{14}F_3NO_6$: C 54.42, H 3.55, F 14.35, N 3.53, O 24.16; found: C 54.41, H 3.54, N 3.51.

The filtrate was acidified with 10% HCl and filtered to yield another white solid, 3-(4-carbamoyl-3-trifluoromethylphenoxy)-5-methoxycarbonylbenzoic acid (0.123 g, 44.8%). M.p. 255 °C; ^{1}H NMR (400 MHz, [D$_6$]DMSO, 25 °C): δ = 13.6 (br, 1H; COO*H*), 8.25 (s, 1H; ArH), 7.99 (s, 1H; NH of amide), 7.74 (s, 1H; ArH), 7.72 (s, 1H; another NH of amide), 7.60 (d, ^1J(H,H) = 8.2 Hz, 2H; ArH), 7.50 (d, ^1J(H,H) = 2.3 Hz, 1H; ArH), 7.39 (dd, ^1J(H,H) = 8.4 Hz, ^2J(H,H) = 2.3 Hz, 1H; ArH), 3.86 ppm (s, 3H; CH_3); ^{13}C NMR (100 MHz, [D$_6$]DMSO, 25 °C): δ = 168.3, 165.7, 164.8, 156.5, 156.2, 133.6, 132.8, 132.2, 128.0 (q, ^2J(C,F) = 32.0 Hz), 125.3, 123.4, 123.1 (q, ^1J(C,F) = 272.5 Hz), 123.0, 122.4, 119.1, 117.3, 52.7 ppm; EIMS: *m/z*: calcd: 383.0617; found: 383.0616 [M^+]; elemental analysis calcd (%) for $C_{17}H_{12}F_3NO_6$: C 53.27, H 3.16, F 14.87, N 3.65, O 25.05; found: C 53.15, H 3.13, N 3.64.

Compound 18: Compound **17** (0.1 g, 0.252 mmol) was dissolved in a solvent mixture of THF (6 mL), methanol (3 mL), and water (1 mL). Lithium hydroxide (0.030 g, 1.258 mmol) was added at 0 °C and stirred for 4 h. The mixture was warmed up to room temperature, and mixed with excess of water. The white suspension was acidified with 10% HCl (aq) and kept in a refrigerator overnight. The white solid was filtered and dried under vacuum (0.086 g, 92.5%). M.p. 120 °C; ^{1}H NMR (400 MHz, [D$_6$]DMSO, 25 °C): δ = 13.2 (br, 2H; COOH), 8.35 (s, 1H; ArH), 7.99 (s, 1H; NH of amide), 7.73 (s, 1H; another NH of amide), 7.66 (d, ^1J(H,H) = 2.3 Hz, 1H; ArH), 7.60 (d, ^1J(H,H) = 8.3 Hz, 1H; ArH), 7.51 (d, ^1J(H,H) = 2.3 Hz, 1H; ArH), 7.39 ppm (dd, ^1J(H,H) = 8.3 Hz, ^2J(H,H) = 2.3 Hz, 1H; ArH); ^{13}C NMR (100 MHz, [D$_6$]DMSO, 25 °C): δ = 168.5, 165.9, 156.5, 156.3, 133.5, 132.8, 131.0, 128.1 (q, ^2J(C,F) = 32.0 Hz), 125.5, 123.8, 123.2 (q, ^1J(C,F) = 272.4 Hz), 122.5, 117.4 ppm (q, ^3J(C,F) = 4.8 Hz); EIMS: *m/z*: calcd: 369.0460; found: 369.0464 [M^+]; elemental analysis calcd (%) for $C_{16}H_{10}F_3NO_6$: C 52.04, H 2.73, F 15.44, N 3.79, O 26.00; found: C 49.59, H 2.95, N 3.61.

Using the same protocol, 3-(4-carbamoyl-3-trifluoromethylphenoxy)-5-methoxycarbonyl benzoic acid was hydrolyzed to also give compound **18**.

Compound 19 (G0-G1): Compound **18** (0.06 g, 0.162 mmol), 1-dodecanol (0.09 mL, 0.406 mmol), and DMAP (0.040 g, 0.325 mol) were dissolved in *N*,*N*-dimethyl formamide (DMF, 12 mL) and placed in a 25 mL one-necked round-bottomed flask. The reaction mixture was stirred at 0 °C for 30 min. EDC (0.062 g, 0.325 mmol) was added into the flask and stirred for an additional 30 min. The reaction mixture was warmed up to room temperature and stirred for 18 h. Then the reaction mixture was filtered, washed with 0.1 M HCl (aq), 0.1 M $NaHCO_3$, and brine. The organic layer was dried and evaporated in a rotary evaporator. The crude product was purified by column chromatography using *n*-hexane as the eluent (0.078 g, 68.2%). M.p. 92 °C; ^{1}H NMR (400 MHz, $CDCl_3$, 25 °C): δ = 8.48 (s, 1H; ArH), 7.84 (s, 2H; ArH), 7.59 (d, ^1J(H,H) = 8.4 Hz, 1H; ArH), 7.32 (d, ^1J(H,H) = 2.3 Hz, 1H; ArH), 7.14 (dd, ^1J(H,H) = 8.4 Hz, ^2J(H,H) = 2.2 Hz, 1H; ArH), 5.90 (d, ^1J(H,H) = 79.5 Hz, 2H; NH of amide), 4.32 (t, ^1J(H,H) = 6.7 Hz, 4H; O=$COCH_2$), 1.75 (m, ^1J(H,H) = 7.0 Hz, 4H; O=$COCH_2CH_2$), 1.24 (m, 32H), 0.85 ppm (t, ^1J(H,H) =

6.4 Hz, 6H; CH_3); ^{13}C NMR (100 MHz, $CDCl_3$, 25 °C): $\delta = 168.8$, 165.0, 158.0, 155.8, 133.2, 131.0, 130.0, 129.8 (q, $^2J(C,F) = 32.6$ Hz), 127.0, 124.5, 122.9 (q, $^1J(C,F) = 272.3$ Hz), 121.1, 116.7 (q, $^3J(C,F) = 5.2$ Hz), 65.9, 32.1, 31.9, 29.6–29.2, 28.6, 25.9, 22.8, 22.7, 14.1 ppm; ESIMS: *m/z*: calcd: 706.4289; found: 706.4319 $[M+H^+]$; elemental analysis calcd (%) for $C_{40}H_{58}F_3NO_6$: C 68.06, H 8.28, F 8.07, N 1.98, O 13.60; found: C 68.62, H 8.49, N 1.93.

PGSE NMR spectroscopy: The diffusion coefficient measurements were carried out using a Bruker AVANCE 400 MHz NMR spectrometer (equipped with a 5 mm Bruker QNP probe with an actively shielded *z* gradient coil) at 25 °C. Diffusion coefficients were extracted from a series of ^1H NMR spectra measured by a stimulated echo sequence using bipolar gradient (STEbp) pulse sequences as a function of gradient amplitude. The diffusion time (Δ) was 100 ms, the length of the gradient (δ) was 2.6 ms and the delay time (d1) was 30 s. At a given concentration, 16 data points with different gradient strengths ranging from 1 to 51 G cm^{-1} were obtained. Using the attenuated intensities of the peak shown at $\delta =$ 1.27 ppm (assigned to methylene groups in the alkyl chain), diffusion coefficients were calculated by using SimFit[38] in Bruker XWINNMR 3.0. Obtained diffusion coefficients were calibrated by measuring the diffusion coefficient of residual chloroform in each sample solution ($D_{solution}$) and comparing it to the chloroform diffusion coefficient in pure $CDCl_3$ (D_{pure}). This allowed an estimation of the solution viscosity of the solution to be made. Equation (1) was used for this calibration:

$$D_{correlated} = D_{obtained} \times (D_{pure}/D_{solution}) \quad (1)$$

Normalization of the diffusion coefficients by the molecular volume of the bis-dendritic gelators was conducted by multiplying the values by the cubed root of the molecular weights of the gelators.

Evaluation of association constants: NMR spectroscopy chemical shifts of the bis-dendritic gelators were obtained on a Bruker AVANCE 300 MHz NMR spectrometer. Based on the models described by Martin,[20] association constants for the DIM model were evaluated by using a nonlinear curve fitting module in Origin 7.0[39] with Equation (2):

$$P = P_\lambda + (P_\alpha - P_\lambda)\frac{-1+\sqrt{1+8K_2C_T}}{4K_2C_T} \quad (2)$$

in which P, C_T, P_α, and P_λ denote the observed chemical shift of the corresponding proton, total concentration in solution, the chemical shift of the proton in the monomeric state, and the chemical shift of the proton in the dimeric state, respectively. K_2, P_α, and P_λ were optimized by using the Levenberg–Marquardt iterative method. Association constants for the EK model were evaluated using this equation, setting $K_E = 2K_2$. Association constants for the coEK model were evaluated by using a custom Python routine provided in the Supporting Information. The chemical shifts of protons on the periphery of aggregates were assumed to be given by Equation (3):

$$P_\lambda = (P_\alpha + P_\xi)/2 \quad (3)$$

in which P_ξ denotes the chemical shift of the proton on the interior of aggregates. Optimization of K_E, ρ, P_α, and P_ξ was performed using Python 2.5[40] with the SciPy and Elefant modules.

Full DSC thermograms of the bis-dendritic gelator molecules, SEM and TEM images of the gels, and the Python script for fitting based on the coEK model can be found in the Supporting Information.

Acknowledgements

M.S. thanks Dr. T. F. A. de Greef for invaluable advice for NMR spectroscopy experiments and Dr. M. Jin for the Python script used in the study. This work was supported by the National Research Foundation (NRF) through ERC (R11-2007-050-04001-0) and NRL (R0A-2008-000-20121-0) programs and by Fundamental R&D program for Core Technology of Materials funded by the Ministry of Knowledge Economy, Republic of Korea.

[1] a) G. R. Newkome, C. N. Moorefield, F. Vögtle, *Dendrimers and Dendrons*, Wiley-VCH, Weinheim, **2001**; b) D. A. Tomalia, A. M. Naylor, W. A. Goddard III, *Angew. Chem.* **1990**, *102*, 119–157; *Angew. Chem. Int. Ed. Engl.* **1990**, *29*, 138–175; c) O. A. Matthews, A. N. Shipway, J. F. Stoddart, *Prog. Polym. Sci.* **1998**, *23*, 1–56; d) M. Fischer, F. Vögtle, *Angew. Chem.* **1999**, *111*, 934–955; *Angew. Chem. Int. Ed.* **1999**, *38*, 884–905; e) A. W. Bosman, H. M. Janssen, E. W. Meijer, *Chem. Rev.* **1999**, *99*, 1665–1688; f) K. Inoue, *Prog. Polym. Sci.* **2000**, *25*, 453–571; g) R. Esfand, D. A. Tomalia, *Drug Discovery Today* **2001**, *6*, 427–436; h) S. M. Grayson, J. M. J. Fréchet, *Chem. Rev.* **2001**, *101*, 3819–3867; i) S. Hecht, J. M. J. Fréchet, *Angew. Chem.* **2001**, *113*, 76–94; *Angew. Chem. Int. Ed.* **2001**, *40*, 74–91; j) L. H. Bryant, Jr., J. W. M. Bulte, *Focus on Biotechnology* **2002**, *7*, 47–69; k) C. C. Lee, J. A. MacKay, J. M. J. Fréchet, F. C. Szoka, *Nat. Biotechnol.* **2005**, *23*, 1517–1526; l) W.-D. Jang, K. M. K. Selim, C.-H. Lee, I.-K. Kang, *Prog. Polym. Sci.* **2009**, *34*, 1–23.

[2] a) F. Zeng, S. C. Zimmerman, *Chem. Rev.* **1997**, *97*, 1681–1712; b) T. Emrick, J. M. J. Fréchet, *Curr. Opin. Colloid Interface Sci.* **1999**, *4*, 15–23; c) F. Vögtle, S. Gestermann, R. Hesse, H. Schwierz, B. Windisch, *Prog. Polym. Sci.* **2000**, *25*, 987–1041; d) G. M. Dykes, *J. Chem. Technol. Biotechnol.* **2001**, *76*, 903–918.

[3] a) V. Percec, P. Chu, G. Ungar, J. Zhou, *J. Am. Chem. Soc.* **1995**, *117*, 11441–11454; V. Percec, G. Johansson, G. Ungar, J. Zhou, *J. Am. Chem. Soc.* **1996**, *118*, 9855–9866; V. Percec, C.-H. Ahn, B. Barboiu, *J. Am. Chem. Soc.* **1997**, *119*, 12978–12979; S. D. Hudson, H.-T. Jung, V. Percec, W.-D. Cho, G. Johansson, G. Ungar, V. S. K. Balagurusamy, *Science* **1997**, *278*, 449–452; V. Percec, C.-H. Ahn, G. Ungar, D. J. P. Yeardley, M. Möller, S. S. Sheiko, *Nature* **1998**, *391*, 161–164; V. Percec, W.-D. Cho, G. Ungar, D. J. P. Yeardley, *Chem. Eur. J.* **2002**, *8*, 2011–2025; J. A. A. W. Elemans, M. J. Boerakker, S. J. Holder, A. E. Rowan, W.-D. Cho, V. Percec, R. J. M. Nolte, *Proc. Natl. Acad. Sci. USA* **2002**, *99*, 5093–5098; V. Percec, M. Glodde, G. Johansson, V. S. K. Balagurusamy, P. A. Heiney, *Angew. Chem.* **2003**, *115*, 4474–4478; *Angew. Chem. Int. Ed.* **2003**, *42*, 4338–4342; b) V. Percec, A. E. Dulcey, V. S. K. Balagurusamy, Y. Miura, J. Smidrkal, M. Peterca, S. Nummelin, U. Edlund, S. D. Hudson, P. A. Heiney, H. Duan, S. N. Magonov, S. A. Vinogradov, *Nature* **2004**, *430*, 764–768; V. Percec, A. E. Dulcey, M. Peterca, P. Adelman, R. Samant, V. S. K. Balagurusamy, P. A. Heiney, *J. Am. Chem. Soc.* **2007**, *129*, 5992–6002; V. Percec, J. Smidrkal, M. Peterca, C. M. Mitchell, S. Nummelin, A. E. Dulcey, M. J. Sienkowska, P. A. Heiney, *Chem. Eur. J.* **2007**, *13*, 3989–4007; V. Percec, M. Peterca, A. E. Dulcey, M. R. Imam, S. D. Hudson, S. Nummelin, P. Adelman, P. A. Heiney, *J. Am. Chem. Soc.* **2008**, *130*, 13079–13094; c) V. Percec, J. G. Rudick, M. Peterca, M. E. Yurchenko, J. Smidrkal, P. A. Heiney, *Chem. Eur. J.* **2008**, *14*, 3355–3362; d) V. Percec, M. R. Imam, M. Peterca, D. A. Wilson, P. A. Heiney, *J. Am. Chem. Soc.* **2009**, *131*, 1294–1304.

[4] a) Y. Wang, F. Zeng, S. C. Zimmerman, *Tetrahedron Lett.* **1997**, *38*, 5459–5462; P. S. Corbin, L. J. Lawless, Z. Li, Y. Ma, M. J. Witmer, S. C. Zimmerman, *Proc. Natl. Acad. Sci. USA* **2002**, *99*, 5099–5104; Y. Ma, S. V. Kolotuchin, S. C. Zimmerman, *J. Am. Chem. Soc.* **2002**, *124*, 13757–13769; b) H.-A. Klok, J. J. Hwang, J. D. Hartgerink, S. I. Stupp, *Macromolecules* **2002**, *35*, 6101–6111; E. R. Zubarev, S. I. Stupp, *J. Am. Chem. Soc.* **2002**, *124*, 5762–5773; S. Lecommandoux, H.-A. Klok, M. Sayar, S. I. Stupp, *J. Polym. Sci. Polym. Chem. Ed.* **2003**, *41*, 3501–3518; J. C. Stendahl, L. Li, R. C. Claussen, S. I. Stupp, *Biomaterials* **2004**, *25*, 5847–5856; c) C.-H. Wong, H.-F. Chow, S.-K. Hui, K.-H. Sze, *Org. Lett.* **2006**, *8*, 1811–1814.

[5] a) M. Lee, Y.-S. Jeong, B.-K. Cho, N.-K. Oh, W.-C. Zin, *Chem. Eur. J.* **2002**, *8*, 876–883; C.-J. Jang, J.-H. Ryu, J.-D. Lee, D. Sohn, M. Lee, *Chem. Mater.* **2004**, *16*, 4226–4231; J. Holzmueller, K. L. Genson, Y. Park, Y.-S. Yoo, M.-H. Park, M. Lee, V. Tsukruk, *Langmuir* **2005**, *21*, 6392–6398; b) B.-K. Cho, A. Jain, S. Mahajan, H. Ow, S. M. Gruner, U. Wiesner, *J. Am. Chem. Soc.* **2004**, *126*, 4070–

4071; c) S. Coco, C. Cordovilla, B. Donnio, P. Espinet, M. J. García-Casas, D. Guillon, *Chem. Eur. J.* **2008**, *14*, 3544–3552.

[6] a) A. P. H. J. Schenning, C. Elissen-Román, J.-W. Weener, M .W. P. L. Baars, S. J. van der Gaast, E. W. Meijer, *J. Am. Chem. Soc.* **1998**, *120*, 8199–8208; b) K. Ariga, T. Urakawa, A. Michiue, Y. Sasaki, J. Kikuchi, *Langmuir* **2000**, *16*, 9147–9150; K. Ariga, T. Urakawa, A. Michiue, J. Kikuchi, *Langmuir* **2004**, *20*, 6762–6769; c) A. R. Schmitzer, S. Franceschi, E. Perez, I. Rico-Lattes, A. Lattes, L. Thion, M. Erard, C. Vidal, *J. Am. Chem. Soc.* **2001**, *123*, 5956–5961; d) D. Joester, M. Losson, R. Pugin, H. Heinzelmann, E. Walter, H. P. Merkle, F. Diederich, *Angew. Chem.* **2003**, *115*, 1524–1528; *Angew. Chem. Int. Ed.* **2003**, *42*, 1486–1490; e) S. V. Aathimanikandan, E. N. Savariar, S. Thayumanavan, *J. Am. Chem. Soc.* **2005**, *127*, 14922–14929; A. Klaikherd, B. S. Sandanaraj, D. R. Vutukuri, S. Thayumanavan, *J. Am. Chem. Soc.* **2006**, *128*, 9231–9237; A. V. Ambade, S. V. Aathimanikandan, D. van der Poll, S. Thayumanavan, *J. Org. Chem.* **2007**, *72*, 8167–8174; f) K. T. Kim, M. A. Winnik, I. Manners, *Soft Matter* **2006**, *2*, 957–965; g) B.-B. Wang, W.-S. Li, X.-R. Jia, M. Gao, L. Jiang, Y. Wei, *J. Polym. Sci. Polym. Chem. Ed.* **2008**, *46*, 4584–4593; h) C. N. Urbani, D. E. Lonsdale, C. A. Bell, M. R. Whittaker, M. J. Monteiro, *J. Polym. Sci. Polym. Chem. Ed.* **2008**, *46*, 1533–1547.

[7] a) J.-F. Nierengarten, J.-F. Eckert, Y. Rio, M. del Pilar Carreon, J.-L. Gallani, D. Guillon, *J. Am. Chem. Soc.* **2001**, *123*, 9743–9748; I. Bury, B. Heinrich, C. Bourgogne, D. Guillon, B. Donnio, *Chem. Eur. J.* **2006**, *12*, 8396–8413; I. Bury, B. Donnio, J.-L. Gallani, D. Guillon, *Langmuir* **2007**, *23*, 619–625; b) A. Kimoto, J.-S. Cho, M. Higuchi, K. Yamamoto, *Macromolecules* **2004**, *37*, 5531–5537; N. R. Luman, M. W. Grinstaff, *Org. Lett.* **2005**, *7*, 4863–4866.

[8] a) I. Gitsov; K. L. Wooley, C. J. Hawker, P. T. Ivanova, J. M. J. Fréchet, *Macromolecules* **1993**, *26*, 5621–5627; K. L. Wooley, C. J. Hawker, P. T. Ivanova, J. M. J. Fréchet, *Macromolecules* **1993**, *26*, 5621–5627; M. R. Leduc, C. J. Hawker, J. Dao, J. M. J. Fréchet, *J. Am. Chem. Soc.* **1996**, *118*, 11111–11118; J. L. Mynar, A. P. Goodwin, J. A. Cohen, Y. Ma, G. R. Fleming, J. M. J. Fréchet, *Chem. Commun.* **2007**, 2081–2082; b) D. J. Pochan, L. Pakstis, E. Huang, C. Hawker, R. Vestberg, *Macromolecules* **2002**, *35*, 9239–9242; c) I. Gitsov, C. Zhu, *J. Am. Chem. Soc.* **2003**, *125*, 11228–11234; K. R. Lambrych, I. Gitsov, *Macromolecules* **2003**, *36*, 1068–1074; I. Gitsov, A. Simonyan, N. G. Vladimirov, *J. Polym. Sci. Polym. Chem. Ed.* **2007**, *45*, 5136–5148.

[9] a) J. Iyer, K. A. Fleming, P. T. Hammond, *Macromolecules* **1998**, *31*, 8757–8765; M. A. Johnson, J. Iyer, P. T. Hammond, *Macromolecules* **2004**, *37*, 2490–2501; P. M. Nguyen, P. T. Hammond, *Langmuir* **2006**, *22*, 7825–7832; b) L. Tian, P. Nguyen, P. T. Hammond, *Chem. Commun.* **2006**, 3489–3491; L. Tian, P. T. Hammond, *Chem. Mater.* **2006**, *18*, 3976–3984; c) H.-I. Lee, J. A. Lee, Z. Poon, P. T. Hammond, *Chem. Commun.* **2008**, 3726–3728.

[10] a) B.-K. Cho, A. Jain, S. M. Gruner, U. Wiesner, *Science* **2004**, *305*, 1598–1601; B.-K. Cho, A. Jain, S. M. Gruner, U. Wiesner, *Chem. Commun.* **2005**, 2143–2145; Y.-W. Chung, J.-K. Lee, W.-C. Zin, B.-K. Cho, *J. Am. Chem. Soc.* **2008**, *130*, 7139–7147; E. Lee, B.-I. Lee, S.-H. Kim, J.-K. Lee, W.-C. Zin, B.-K. Cho, *Macromolecules* **2009**, *42*, 4134–4140; b) T. M. Chapman, G. L. Hillyer, E. J. Mahan, K. A. Shaffer, *J. Am. Chem. Soc.* **1994**, *116*, 11195–11196; c) Z. Ge, D. Chen, J. Zhang, J. Rao, J. Yin, D. Wang, X. Wan, W. Shi, S. Liu, *J. Polym. Sci. Polym. Chem. Ed.* **2007**, *45*, 1432–1445; d) A. Sousa-Herves, E. Fernandez-Megia, R. Riguera, *Chem. Commun.* **2008**, 3136–3138; e) A. Harada, K. Nakanishi, S. Ichimura, C. Kojima, K. Kono, *J. Polym. Sci. Polym. Chem. Ed.* **2009**, *47*, 1217–1223; f) S.-J. Hsieh, C.-C. Wang, C.-Y. Chen, *Macromolecules* **2009**, *42*, 4787–4794.

[11] a) J. H. Fuhrhop, W. Helfrich, *Chem. Rev.* **1993**, *93*, 1565–1582; b) P. Terech, R. G. Weiss, *Chem. Rev.* **1997**, *97*, 3133–3159; c) O. Gronwald, E. Snip, S. Shinkai, *Curr. Opin. Colloid Interface Sci.* **2002**, *7*, 148–156; d) A. R. Hirst, D. K. Smith, *Top. Curr. Chem.* **2005**, *256*, 237–273; D. K. Smith, *Chem. Commun.* **2006**, 34–44; D. K. Smith, *Adv. Mater.* **2006**, *18*, 2773–2778.

[12] a) W.-D. Jang, T. Aida, *Macromolecules* **2003**, *36*, 8461–8469; b) V. Percec, M. Peterca, M. E. Yurchenko, J. G. Rudick, P. A. Heiney, *Chem. Eur. J.* **2008**, *14*, 909–918; c) J. H. Kim, M. Seo, Y. J. Kim, S. Y. Kim, *Langmuir* **2009**, *25*, 1761–1766; d) Y. Chen, Y. Lv, Y. Han, B. Zhu, F. Zhang, Z. Bo, C.-Y. Liu, *Langmuir* **2009**, *25*, 8548–8555.

[13] a) M. McWatt, G.-J. Boons, *Euro. J. Org. Chem.* **2001**, 2535–2545; b) C. Kim, K. T. Kim, Y. Chang, *J. Am. Chem. Soc.* **2001**, *123*, 5586–5587; H. S. Ko, C. Park, S. M. Lee, H. H. Song, C. Kim, *Chem. Mater.* **2004**, *16*, 3872–3876; c) H.-F. Chow, J. Zhang, *Chem. Eur. J.* **2005**, *11*, 5817–5831; H.-F. Chow, J. Zhang, *Tetrahedron* **2005**, *61*, 11279–11290.

[14] a) Y. Kamikawa, T. Kato, *Langmuir* **2007**, *23*, 274–278; b) Y. Ji, Y. F. Luo, X.-.R. Jia, E.-Q. Chen, Y. Huang, C. Ye, B.-B. Wang, Q.-F. Zhou, Y. Wei, *Angew. Chem.* **2005**, *117*, 6179–6183; *Angew. Chem. Int. Ed.* **2005**, *44*, 6025–6029; W.-S. Li, X.-R. Jia, B.-B. Wang, Y. Ji, Y. Wei, *Tetrahedron* **2007**, *63*, 8794–8800; M. Gao, G.-C. Kuang, X.-R. Jia, W.-S. Li, Y. Li, Y. Wei, *Tetrahedron Lett.* **2008**, *49*, 6182–6187; c) M. Yang, Z. Zhang, F. Yuan, W. Wang, S. Hess, K. Lienkamp, I. Lieberwirth, G. Wegner, *Chem. Eur. J.* **2008**, *14*, 3330–3337; Z. Zhang, M. Yang, X. Zhang, L. Zhang, B. Liu, P. Zheng, W. Wang, *Chem. Eur. J.* **2009**, *15*, 2352–2361.

[15] a) K. S. Partridge, D. K. Smith, G. M. Dykes, P. T. McGrail, *Chem. Commun.* **2001**, 319–320; A. R. Hirst, D. K. Smith, M. C. Feiters, H. P. M. Geurts, A. C. Wright, *J. Am. Chem. Soc.* **2003**, *125*, 9010–9011; A. R. Hirst, D. K. Smith, M. C. Feiters, H. P. M. Geurts, *Langmuir* **2004**, *20*, 7070–7077; A. R. Hirst, D. K. Smith, M. C. Feiters, H. P. M. Geurts, *Chem. Eur. J.* **2004**, *10*, 5901–5910; A. R. Hirst, D. K. Smith, J. P. Harrington, *Chem. Eur. J.* **2005**, *11*, 6552–6559; b) C. S. Love, A. R. Hirst, V. Chechik, D. K. Smith, I. Ashworth, C. Brennan, *Langmuir* **2004**, *20*, 6580–6585; J. G. Hardy, A. R. Hirst, D. K. Smith, C. Brennan, I. Ashworth, *Chem. Commun.* **2005**, 385–387; B. Huang, A. R. Hirst, D. K. Smith, V. Castelletto, I. W. Hamley, *J. Am. Chem. Soc.* **2005**, *127*, 7130–7139; c) A. R. Hirst, B. Huang, V. Castelletto, I. W. Hamley, D. K. Smith, *Chem. Eur. J.* **2007**, *13*, 2180–2188.

[16] a) Q. Liu, H. Zang, S. Yin, L. Wu, C. Shao, Z. Su, *Polymer* **2007**, *48*, 3759–3770; b) Y. Feng, Z.-T. Liu, J. Liu, Y.-M. He, Q.-Y. Zheng, Q.-H. Fan, *J. Am. Chem. Soc.* **2009**, *131*, 7950–7951.

[17] a) E. R. Zubarev, M. U. Pralle, E. D. Sone, S. I. Stupp, *J. Am. Chem. Soc.* **2001**, *123*, 4105–4106; E. R. Zubarev, M. U. Pralle, E. D. Sone, S. I. Stupp, *Adv. Mater.* **2002**, *14*, 198–203; E. D. Sone, E. R. Zubarev, S. I. Stupp, *Small* **2005**, *1*, 694–697; E. R. Zubarev, E. D. Sone, S. I. Stupp, *Chem. Eur. J.* **2006**, *12*, 7313–7327; b) B. W. Messmore, J. F. Hulvat, E. D. Sone, S. I. Stupp, *J. Am. Chem. Soc.* **2004**, *126*, 14452–14458; B. W. Messmore, P. A. Sukerkar, S. I. Stupp, *J. Am. Chem. Soc.* **2005**, *127*, 7992–7993; c) J. C. Stendahl, L. Li, E. R. Zubarev, Y.-R. Chen, S. I. Stupp, *Adv. Mater.* **2002**, *14*, 1540–1543.

[18] a) M. Mammen, S. K. Choi, G. M. Whitesides, *Angew. Chem.* **1998**, *110*, 2908–2953; *Angew. Chem. Int. Ed.* **1998**, *37*, 2754–2794; b) A. Varki, *Glycobiology* **1993**, *3*, 97–130.

[19] a) C. Valério, J.-L. Fillaut, J. Ruiz, J. Guittard, J.-C. Blais, D. Astruc, *J. Am. Chem. Soc.* **1997**, *119*, 2588–2589; b) H.-F. Chow, C.-F. Leung, G.-X. Wang, Y.-Y. Yang, *C. R. Chim.* **2003**, *6*, 735–745; c) S. Hong, P. R. Leroueil, I. J. Majoros, B. G. Orr, J. R. Baker, Jr., M. M. B. Holl, *Chem. Biol.* **2007**, *14*, 107–115; d) T. Kehat, M. Portnoy, *Chem. Commun.* **2007**, 2823–2825; e) G. Zaupa, P. Scrimin, L. J. Prins, *J. Am. Chem. Soc.* **2008**, *130*, 5699–5709.

[20] R. B. Martin, *Chem. Rev.* **1996**, *96*, 3043–3064.

[21] a) B. Bai, H. Wang, H. Xin, F. Zhang, B. Long, X. Zhang, S. Qu, M. Li, *New J. Chem.* **2007**, *31*, 401–408; S. Qu, M. Li, *Tetrahedron* **2008**, *64*, 10890–10895; b) J. E. A. Webb, M. J. Crossley, P. Turner, P. Thordarson, *J. Am. Chem. Soc.* **2007**, *129*, 7155–7162; c) A. R. Hirst, I. A. Coates, T. R. Boucheteau, J. F. Miravet, B. Escuder, V. Castelletto, I. W. Hamley, D. K. Smith, *J. Am. Chem. Soc.* **2008**, *130*, 9113–9121.

[22] A. Nanjia, G. R. Desiraju, *Top. Curr. Chem.* **1998**, *198*, 58–95.

[23] a) M. C. Etter, *Acc. Chem. Res.* **1990**, *23*, 120–126; b) M. C. Etter, *J. Phys. Chem.* **1991**, *95*, 4601–4610.

[24] U. Beginn, S. Sheiko, M. Möller, *Macromol. Chem. Phys.* **2000**, *201*, 1008–1015.
[25] a) M. Seo, G. Seo, S. Y. Kim, *Angew. Chem.* **2006**, *118*, 6454–6458; *Angew. Chem. Int. Ed.* **2006**, *45*, 6306–6310; b) M. Seo, J. H. Kim, G. Seo, C.-H. Shin, S. Y. Kim, *Chem. Eur. J.* **2009**, *15*, 612–622.
[26] M. Seo, B. J. Beck, J. M. J. Paulusse, C. J. Hawker, S. Y. Kim, *Macromolecules* **2008**, *41*, 6413–6418.
[27] C. J. Hawker, J. M. J. Fréchet, *J. Am. Chem. Soc.* **1990**, *112*, 7638–7647.
[28] a) M. Seredyuk, A. B. Gaspar, V. Ksenofontov, S. Reiman, Y. Galyametdinov, W. Haase, E. Rentschler, P. Gütlich, *Chem. Mater.* **2006**, *18*, 2513–2519; b) C. Röger, M. G. Muller, M. Lysetska, Y. Miloslavina, A. R. Holzwarth, F. Würthner, *J. Am. Chem. Soc.* **2006**, *128*, 6542–6543.
[29] a) B. C. Smith, *Infrared Spectral Interpretation: A Systematic Approach*, CRC Press, Hamilton, **1999**, p. 128; b) P. G. Puranik, K. V. Ramiah, *Nature* **1961**, *191-192*, 796–797; c) A. V. Iogansen, G. A. Kurkchi, L. A. Dement′eva, *J. Struct. Chem.* **1978**, *18*, 589–595; A. V. Iogansen, G. A. Kurkchi, L. A. Dement′eva, *J. Struct. Chem.* **1978**, *18*, 595–599.
[30] M. Masuda, V. Vill, T. Shimizu, *J. Am. Chem. Soc.* **2000**, *122*, 12327–12333.
[31] a) H. Ihm, J. S. Ahn, M. S. Lah, Y. H. Ko, K. Paek, *Org. Lett.* **2004**, *6*, 3893–3896; b) M. S. Kaucher, Y.-F. Lam, S. Pieraccini, G. Gottarelli, J. T. Davis, *Chem. Eur. J.* **2005**, *11*, 164.
[32] For evaluation of association constants of dendrimers, see a) F. Osterod, A. Kraft, *Chem. Commun.* **1997**, 1435–1436; A. Kraft, F. Osterod, *J. Chem. Soc. Perkin Trans. 1* **1998**, 1019–1025; b) W. Zhang, S. O. Gonzalez, E. Simanek, *Macromolecules* **2002**, *35*, 9015–9021.
[33] J. Zhu, J.-B. Lin, Y.-X. Xu, X.-B. Shao, X.-K. Jiang, Z.-T. Li, *J. Am. Chem. Soc.* **2006**, *128*, 12307–12313.
[34] a) D. Zhao, J. S. Moore, *Org. Biomol. Chem.* **2003**, *1*, 3471–3491; b) T. F. A. de Greef, E. W. Meijer, *Nature* **2008**, *453*, 171–173; c) C. A. Hunter, H. L. Anderson, *Angew. Chem.* **2009**, *121*, 7624–7636; *Angew. Chem. Int. Ed.* **2009**, *48*, 7488–7499.
[35] Comparison of two models was performed by GraphPad QuickCalcs provided on the website (http://www.graphpad.com/quickcalcs/AIC1.cfm). Refer to H. J. Motulsky, A. Christopoulos, Fitting Models to Biological Data Using Linear and Nonlinear Regression: A Practical Guide to Curve Fitting, GraphPad Software Inc., San Diego, CA, **2003**.
[36] a) A. Mulder, J. Huskens, D. N. Reinhoudt, *Org. Biomol. Chem.* **2004**, *2*, 3409–3424; b) J. W. Steed, J. L. Atwood, *Supramolecular Chemistry*, Wiley, New York, **2005**, p. 10; c) L. Baldini, A. Casnati, F. Sansone, R. Ungaro, *Chem. Soc. Rev.* **2007**, *36*, 254–266.
[37] J. Wu, A. Fechtenktter, J. Gauss, M. D. Watson, M. Kastler, C. Fechtenktter, M. Wagner, K. Müllen, *J. Am. Chem. Soc.* **2004**, *126*, 11311–11321.
[38] SimFit integrated in XWINNMR 3.0, Bruker Biospin GmbH, Reinstetten.
[39] Origin 7.0, OriginLab, Northampton, MA.
[40] Python 2.5, G. Von Rossum, Python Software Foundation, http://www.python.org.

Received: September 18, 2009
Published online: January 11, 2010

